Karl Christian Lautenschläger

Suitability of Modern Wi-Fi for Wireless-Infield-Communication of Agricultural Machines

Diploma Thesis in Information Systems Engineering

20 March 2023

Please cite as:
Karl Christian Lautenschläger, “Suitability of Modern Wi-Fi for Wireless-Infield-Communication of Agricultural Machines,”
Diploma Thesis (Diplomarbeit), Faculty of Computer Science, TU Dresden, Germany, March 2023.

TECHNISCHE UNIVERSITÄT DRESDEN

Networked Systems Modeling
Faculty of Computer Science, TU Dresden

Nöthnitzer Str. 46 · 01187 Dresden · Germany

https://nsm.inf.tu-dresden.de/

Suitability of Modern Wi-Fi for Wireless-Infield-Communication of Agricultural Machines

Diploma Thesis in Information Systems Engineering

vorgelegt von

Karl Christian Lautenschläger

geb. am 29. Juni 1998
in Magdeburg

angefertigt an der

Technischen Universität Dresden
Fakultät Informatik
Networked Systems Modeling

Betreuer:	**Christoph Sommer**
Gutachter:	**Christoph Sommer**
	Burkhard Hensel
Abgabe der Arbeit:	**20. März 2023**

Erklärung

Ich versichere, dass ich die Arbeit ohne fremde Hilfe und ohne Benutzung anderer als der angegebenen Quellen angefertigt habe und dass die Arbeit in gleicher oder ähnlicher Form noch keiner anderen Prüfungsbehörde vorgelegen hat und von dieser als Teil einer Prüfungsleistung angenommen wurde.
Alle Ausführungen, die wörtlich oder sinngemäß übernommen wurden, sind als solche gekennzeichnet.

Declaration

I declare that the work is entirely my own and was produced with no assistance from third parties.
I certify that the work has not been submitted in the same or any similar form for assessment to any other examining body and all references, direct and indirect, are indicated as such and have been cited accordingly.

(Karl Christian Lautenschläger)
Dresden, 20 March 2023

This template is for use with `pdflatex` and `biber`. It has been tested with TeX Live 2020 (as of 25 Oct 2020).

Abstract

about 1/2 page:

1. Motivation (Why do we care?)
2. Problem statement (What problem are we trying to solve?)
3. Approach (How did we go about it)
4. Results (What's the answer?)
5. Conclusion (What are the implications of the answer?)

The abstract is a miniature version of the thesis. It should be treated as an entirely separate document. Do not assume that a reader who has access to an abstract will also have access to the thesis. Do not assume that a reader who reads the thesis has read the abstract.

Kurzfassung

Gleicher Text (sinngemäß, nicht wörtlich) in Deutsch

Contents

The table of contents should fit on one page. When in doubt, adjust the `tocdepth` counter.

Chapter 1

Introduction

- general motivation for your work, context and goals.
- context: make sure to link where your work fits in
- problem: gap in knowledge, too expensive, too slow, a deficiency, superseded technology
- strategy: the way you will address the problem
- recommended length: 1-2 pages.

With the growing demand for increased efficiency and autonomy in the agricultural domain, Wireless-Infield Communication (WIC) has emerged as a key technology to increase the automation and digitalization of agricultural processes. WIC describes a wireless connection between agricultural machines in the field that enables the exchange of process data.

Given that there are many different agricultural technology companies worldwide, and a mix of their machines often cooperate in the individual agricultural company, demand for interoperability between agricultural machines of different brands has emerged. In 2008, the Agricultural Industry Electronics Foundation (AEF) was founded to develop and standardize this interoperability [1].

The AEF has defined a binary unit system, the ISO 11783 standard, for agricultural machinery communication, mainly tractors and implements [1]. According to Schlingmann and Benishek [2], the ISO 11783 standard is known as the ISOBUS system.

The authors mention that the AEF is currently working on other issues. Among them is also WIC. The associated project group WIC develops and standardizes solutions for Machine-To-Machine (M2M) wireless communication between cooperating agricultural machines.

[1] https://www.aef-online.org/about-us/about-the-aef.html Accessed: 24.07.2022

In order to implement WIC, the WIC project group has been searching for a suitable technology that can realize the required data rates, latencies, robustness, and high transmission range. The plans to implement WIC are written down by members of the WIC project group in [3]. The authors consider the fundamental use of cellular networks as very problematic because, according to [4], only 30 % of the land surface has network coverage. For this reason, one major concern is that the required data cannot be exchanged because there is no network connectivity around many fields. Nevertheless, the authors want to leave the future WIC system open to cellular standards.

The authors' current focus is on Wi-Fi technologies, which must first be evaluated for use in the agricultural environment.

In my final thesis, I indend to support the progress of the WIC project group and investigate how modern Wi-Fi can enable WIC. In particular, I will focus on the current Wi-Fi standard, IEEE 802.11ax. During my research, I will study the use cases of WIC in agriculture and the requirements and challenges for WIC in agriculture. In order to analyze the suitability of IEEE 802.11ax to enable WIC, I will concentrate on the example use cases Agricultural Platooning Service and Video Streaming Service. Agricultural Platooning Service enables the exchange of process data to guide a vehicle in a platoon with a lateral and longitudinal offset to a leading vehicle. Video Streaming Services exchange video data to enable the driver to see the remote content of screens and cameras of other vehicles in the field.

In the beginning, I will analyze agricultural process data to find the requirements and challenges of the mentioned use cases. I will complement these with insights from past research on WIC in agriculture and wireless technologies in the agriculture domain in general.

The suitability of IEEE 802.11ax for WIC depends on whether the required data rates, latencies, robustness, high transmission ranges, and robustness in the harsh agricultural environment can be achieved.

By understanding past limitations of Wi-Fi technologies for outdoor communication networks and exploring how IEEE 802.11ax addresses these limitations, I will investigate how IEEE 802.11ax can be configured. For this purpose, I will first simulate how the capabilities of IEEE 802.11ax affect the data rate and the robustness of the wireless connection. After learning suitable parameter settings for the physical and MAC layer of IEEE 802.11ax, I will simulate the use cases Agricultural Platooning Service and Video Streaming Service to determine whether the requirements and challenges of the WIC use cases can be met by IEEE 802.11ax.

Add Field experiments to the thesis plan.

Chapter 2

Fundamentals

- describe methods and techniques that build the basis of your work
- include what's needed to understand your work (e.g., techniques, protocols, models, hardware, software, ...)
- exclude what's not (e.g., anything you yourself did, anything your reader can be expected to know, ...)
- review related work(!)
- recommended length: approximately one third of the thesis.

2.1 Wireless-Infield Communication

Since 2014, the WIC project group has been working on the development of a for WIC standard, which covers a standard for machine-to-machine communication, encryption, and security [2]. Schlingmann and Benishek [2] summarize the goals of the WIC project team as follows:

- Define use cases for WIC in agriculture
- Evaluate the suitability of communication technologies
- Find suitable communication protocols
- Standardize the WIC common software library
- Develop functional and security requirements and concepts
- Test first prototypes in regards of cross-brand comformance

[2] https://www.aef-online.org/about-us/teams.html

- Write a application guideline

First steps have already been taken in this direction. The use cases and key scenarios are defined and explained by the authors as follows:

- **Real-Time Machine-to-Machine Control** is the exchange of control data under real-time conditions with defined latency policies. This use case enables leader-follower scenarios where agricultural machines follow a leading agricultural machine at a lateral and longitudinal distance. Throughout this thesis, I will refer to Real-Time Machine-to-Machine Control as Agricultural Platooning Service.

- **Streaming Services** are communications that stream video from remote cameras and monitors at a high data rate and low latency. The authors estimate the distance between the communication participants to be less than 100 m. As a result, this data is available on another agricultural vehicle and can be analyzed and processed there. I will refer to Streaming Services as Agricultural Streaming Services in this thesis.

- **Process Data Exchange** describes the exchange of process data. One example is the exchange of already sprayed field areas to prevent multiple spraying of fertilizers and pesticides on the same field area by different machines. According to the authors, this WIC use case requires long-range technologies because agricultural fields worldwide can be vast.

- **Fleet Management & Logistics** is the potential retrieval of data from the ongoing agricultural process. This information can influence economic or agronomic decisions of agricultural enterprises or service companies and is therefore required in a Farm Management Information System (FMIS). Since not all agricultural machines may be connected to the FMIS, the WIC project group is looking at how to use M2M communications to bridge the missing communications infrastructure until the data reaches a machine that can connect to the FMIS.

- **Road Safety** describes a use case which is already a project between the European Telecommunication Standard Institute and the AEF. Since agricultural vehicles are repeatedly underestimated in their size and speed by other road users when they suddenly turn off the field onto the road, the other road users need to be warned in this situation. In this way, smart technologies in cars and motorcycles can brake these vehicles in advance and prevent possible accidents.

Considering that I investigate the Suitability of modern Wi-Fi for Wireless-Infield-Communication and mordern Wi-Fi like Wi-Fi 6 is no long range technologies, I will focus on investigating the suitability of these two Wi-Fi standards for the WIC use cases Real-Time Machine-to-Machine Control and Streaming Services. Throughout this thesis, I will refer to real-time machine-to-machine control as Agricultural Platooning. An example how farmers can benefit from Streaming Services or Agricultural Platooning Services is the corn harvesting and loading process.

2.2 Harvest and Loading Processes as Use Cases for Wireless-Infield Communication

The Forage harvester has proven to be an essential agricultural machine for harvesting and loading forage. Seifert, Grimm, and Schurig [5] define a forage harvester as an agricultural loading machine for nearly all types of animal feed. According to the authors, a forage harvester can load the following animal feed by mounting different cutting and loading devices: Hey, Straw, Corn, Grass and Clover.

In the harvesting and loading process, a Transport Machine (TM) typically drives alongside or behind the Forage Harvester (FH) so that the FH can load the harvested goods onto the trailer of the TM using the spout. Drivers operate both machines and try to keep the speed and distance so that the spout only throws the harvested goods into the trailer of the TM. An image of a corn harvesting and loading process can be seen in Figure 2.1.

Taking a corn harvest scenario as an example, some key figures are represented in [6], a standard reference book in agricultural literature. This book contains key figures of agricultural processes, which 80 experts have compiled. The key figures, which are shown in Table 2.1, are dependent on the Plant Density (PD) and show the large amount of forage harvested by a FH every hour.

Figure 2.1 – Forage Harvester (FH) and Transport Machine (TM) in a corn harvesting and loading process

Plant Density (PD)	20 t/ha	30 t/ha	50 t/ha
Required Transport Machines	5	7	10
Harvested volume in m^3/h	285.7-333.3	428.6-500.0	595.7-695.0
Filled Transport Machine loads in 1/h	5.7 - 6.7	8.6 - 10.0	11.9 - 13.9
Harvested mass in t/h	100	150	208.5

Table 2.1 – Key figures of corn harvest of a Forage Harvester (FH) with a working width of 6.2 m in a 80 ha-field in regards to Plant Density (PD) [6]

The harvesting and loading processes are examples of the use of agricultural Platooning Services as described by Zhang et al. [7]. This Platooning Service creates a leader and follower system where an uncrewed agricultural machine follows a leading operated agricultural machine. The operated FH, as a leader, sets the path and speed and transmits the data via WIC to the TM. Based on the path and speed data of the FH, TM follows unmanned with a longitudinal and lateral offset, as Figure 2.2 displays.

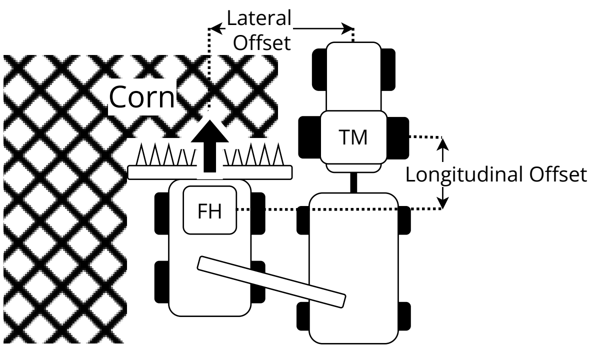

Figure 2.2 – Lateral and longitudinal offset between the two agricultural machines Forage Harvester (FH) and Transport Machine (TM) in a corn harvest scenario

The application of platooning services offers many advantages. The TM is positioned optimally to the FH so that the forage can be loaded ideally from the FH onto the TM.

Because, as displayed in Figure 2.3, fewer and fewer workers are working in agriculture, platooning services for harvest and loading processes can save and free up labour for other activities [8]. As stated in Table 2.1, ten drivers for the TMs are needed in the corn harvest process with a high PD. Using an agricultural Platooning Service, each TM can drive unmanned in the field, leading to fewer workers needed in the corn harvest process.

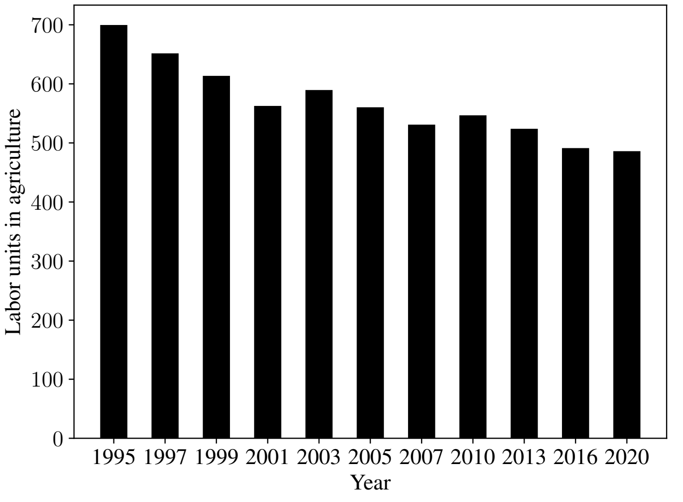

Figure 2.3 – Decrease in the agricultural labor force in Germany based on the data from [9]

Smolnik and Lücke [10] adds that platooning services at the platoon level can reduce FH drivers' workload so that they can focus on optimally adjusting the machines. In addition, TMs can be guided to the FHs in a targeted manner so that logistics processes in the field can be improved.

At the same time, the harvest and loading processes are examples of the video streaming WIC use case, where a video of the TM's filllevel is available at the FH and could be transmitted to the TM in order to inform the TM driver about the machines filllevel. During these harvest and loading processes, the spout of the FH must be controlled to set the loading position of the forage into the trailer of the TM.

According to Murcia [11], different spout guidance and control systems have been developed to automate the filling of the trailer. Spout guidance and control systems use a camera attached to the spout to determine the fill volume at each point of the trailer via machine vision and set the spout to fill the empty parts accordingly. The author describes Autofill - systems from Claas and Intellifill - systems from CNH Industrial as examples of spout guidance systems.

Streaming the video of a camera at the spout from the FH to the TM would be a practical application of the video streaming use case in the harvesting process. If the TM driver can watch a live stream of the trailer's fill level, he will always be informed and knows when the trailer is full and can drive the forage back to the farm.

2.3 Wireless Lans according to IEEE 802.11

Paper Christoph Sommer, Doktorarbeit, Diplomarbeit, Mario Franke, Tobias Hardes

According to Kauffels [12] the first version of the Standard IEEE 802.11 was published in 1999 to enable a wireless alternative to Ethernet - or Token-Ring - networks. Sauter [13] considers IEEE 802.11 also to be an implementation of Ethernet with the help of wirless radio technologies. The author lists the extensions to the original standard, which range from 802.11b, 802.11g, 802.11a, 802.11n, 802.11ac to the latest enhancement 802.11ax. The different IEEE 802.11 standards can operate in the 2.4 GHz - , 5 GHz and 6 GHz - frequency band. IEEE 802.11n is also known as High-Throughput (HT) Wi-Fi, IEEE 802.11ac as Very-High-Throughput (VHT) Wi-Fi [46] and IEEE 802.11ax as High-Efficiency (HE) Wi-Fi [17]. The standards are known by these names. In addition, they are also called Wi-Fi 4, Wi-Fi 5 and Wi-Fi 6 respectively. Jacob et al. [14] fügt dazu noch hinzu, dass es zusätzlich noch die zwei Erweiterungen IEEE 802.11p and dessen Nachfolger IEEE 802.11bd gibt. Diese operieren in einem reservierten Frequency spectrum for Vehicle-to-everything (V2X) nach den Autoren im 5.9 GHz frequency spectrum

Kauffels [12] defines the following three basic architectures for IEEE 802.11.

If two or more stations communicate directly without an AP, they form an ad hoc network. According to the author, this can be set up quickly and easily and is also called Independent Basic Service Set (IBSS).

The Infrastructure Basic Service Set (BSS) mode allows all stations within the range of defined range around the Access Point (AP) to communicate via a central AP. Within the area of the BSS, all stations can move freely and communicate with one another.

Since an AP has limited range and can only cover a certain area, the Extended Service Set (ESS) was introduced. It contains a distribution system, which links several BSS with each other.

Thereby, the BSS coverage areas can physically overlap so that continuous connection of stations within the ESS can be provided. For a better performance the BSS can be placed physically on top of each other. One can also have physically separate BSSs so that these BSSs can be linked together over long distances. According to the author, the standard does not specify a distance limit for such connections.

He also mentions, that the standard defines the following three mobility types for station in an ESS, where a station can do no-transition and thereby stay within a BSS, BSS-transitioning and move from one BSS to another BSS within the same ESS and ESS-transition, where the Station moves from a ESS to another one but no stable connection can be guaranteed.

Sauter [13] adds, that usually Ethernet is used to link APs in within an ESS. But according to the author this can be replaced by a wireless connection, which is called wireless bridge.

ESS not needed?

Sauter 2022 Ad-Hoc Infos

Wi-Fi Physical Layer

The further development of IEEE 802.11 is accompanied by a constant change of the physical layer. Sauter [13] mentions, that all new enhancements of the physical layer of IEEE 802.11 are backward compatible to previous definitions of the it.

According to the Author, IEEE 802.11 initially used DSSS and FHSS as modulation methods. Since IEEE 802.11g the modulation method Orthogonal Frequency-Division Multiplexing (OFDM) can be used in the 2.4 GHz frequency band. The author explains OFDM as following. OFDM divides the transmission channel in subcarriers with different amplitudes, frequencies and phases. Each subcarrier is orthogonal to another one, as they send the information “Low", where only one other subcarrier is sending the information “High".

Symbol length

The data is then sent as OFDM symbols over the individual OFDM subcarriers. The distance between the “Highs" of the subcarriers is specified as subcarrier spacing and corresponds to the reciprocal symbol length. This has now increased from 3.2 µs for IEEE 802.11n to a maximum of 12.8 µs for IEEE 802.11ax [13]. This corresponds to a subcarrier spacing of 312.5 kHz and 78.125 kHz respectively [13].

For the IEEE 802.11p and IEEE 802.11bd standards, a symbol length of 6.4 µs applies, corresponding to a subcarrier spacing of 156.25 kHz [14].

For the modulation and demodulation of the transmitting bits the FFT and IFFT are used respectively. With the reduction of the subcarrier spacing, more subcarriers are created in the transmission channel, so that the FFT size must be increased.

Kauffels [12] adds, that OFDM can be used in the 5 GHz frequency band since IEEE 802.11a.

bandwidth (BW)

Bandwidth is the frequency range of a signal. The bandwidth of a signal is defined as the difference between the highest and lowest frequency of the signal. Kauffels [12] mentions that the bandwidth of a signal is usually specified in or . The bandwidth of a signal is also called the bandwidth of a signal. Kauffels [12] mentions that the bandwidth of a signal is usually specified in or . The bandwidth of a signal is also called the bandwidth of a signal. Kauffels [12] mentions that the bandwidth of a signal is usually specified in or . The bandwidth of a signal is also called the bandwidth of a signal. Kauffels [12] mentions that the bandwidth of a signal is usually specified in or . The bandwidth of a signal is also called the bandwidth of a signal. Kauffels [12] mentions that the bandwidth of a signal is usually specified in or . The bandwidth of a signal is also called the bandwidth of a signal. Kauffels [12] mentions that the bandwidth of a signal is usually specified in or . The bandwidth of a signal is also called the bandwidth of a signal. Kauffels [12] mentions that the bandwidth of a signal is usually specified in or . The bandwidth of a signal is also called the bandwidth of a signal. Kauffels [12] mentions that the bandwidth of a signal is usually specified in or . The bandwidth of a signal is also called the bandwidth of a signal. Kauffels [12] mentions that the bandwidth of a signal is usually specified in or . The bandwidth of a signal is also called the bandwidth of a signal. Kauffels [12] mentions that the bandwidth of a signal is usually specified in

Modulation and Coding Scheme (MCS)

In order to encode as many bits as possible on one OFDM symbol, different MCSs can be used. These MCSs for the IEEE 802.11 standards are based on Phase Shift Keying (PSK) or Quadrature Amplitude Modulation (QAM). [12]. The smallest MCS is binary PSK and encodes 1 bit per symbol. IEEE 802.11ax has the most complex MCS of 256-QAM IEEE 802.11ac to 1024-QAM and thus now encodes 10 bit per symbol [15]. In the V2X range, so can MCSs from binary-PSK to 256-QAM.

In order to encode as many bits as possible on one OFDM symbol, different MCSs can be used. The MCSs for the IEEE 802.11 standards are based on PSK or QAM. [12]. The smallest MCS is Binary - PSK and encodes 1 bit per symbol. IEEE 802.11ax has the most complex MCS of 256 - QAM IEEE 802.11ac to 1024 - QAM and thus now encodes 10 bit per symbol [15]. In the V2X range, so can MCSs from binary-PSK to 256- QAM.

An imaginary, theoretical transmission channel is usually specified as a square-wave signal in the frequency domain with the limits of both minimum and maximum amplitude and cut-off frequency. Kauffels [12] defines the roll-off factor as a cosine-shaped flattening of the square signal between 0 and 1. In addition, the author points out that QAM can generate high roll-off factors, so that signals interfere significantly more with adjacent channels.

In this regards the author recommends setting the parameters in an OFDM system in such a way that first the coding rate and then the complexity of the MCS is reduced in difficult transmission environments. The more bits a MCS encodes on a symbol, the more error-prone the correct decoding of the symbol.

Forward Error Correction (FEC)

Nevertheless bit errors can occur during the transmission. In this regard, [12] mentions and explains FEC as a technique to reduce bit errors during transmission. FEC adds redundant bits to the data. The receiver uses these redundant bits to check the integrity or correct errors of the received data. The proportion of non-redundant transmission bits is defined in the Coding Rate (CR).

To achieve this, binary convolutional coding (BCC) is used mandatory since the IEEE 802.11n standard [15] [16]. Syafei et al. [16] add that it is optionally possible to use low-density parity-check (LDPC). The authors state that LDPC can achieve a better channel capacity performance. This is also confirmed by Afaqui, Garcia-Villegas, and Lopez-Aguilera [15], who point out that LDPC also generates higher computational cost.

IEEE 802.11ax stations must support LDPC when using on the IEEE 802.11ax standard under the following conditions [15] [17]:

- The used bandwidth is greater than 20 MHz
- The chosen MCS is 1024-QAM
- More then four transmission channels are used for the transmission.

IEEE 802.11ax achieves CR of 1/2, 2/3, 3/4, and 5/6 [17]. Similarly, IEEE 802.11p uses the BCC technique, which has been superseded by LDPC in its successor IEEE 802.11ax [14] [18]. Yacheur, Ahmed, and Mosbah [18] argue that this step was important, as LDPC offers better error correction possibilities for higher communication ranges greater than 50 m.

Together with the MCS, the FEC CR form a physical layer specification. This is named after the standard and includes the possible expressions for MCS values and CR of the standard. For IEEE 802.11ax, this results in the HE-MCS index values in Table 2.2

HE-MCS index	Modulation and Coding Scheme (MCS)	Coding Rate (CR)
0	Binary PSK	1/2
1	Quadrature PSK	1/2
2	Quadrature PSK	3/4
3	16-QAM	1/2
4	16-QAM	3/4
5	64-QAM	2/3
6	64-QAM	3/4
7	64-QAM	5/6
8	256-QAM	3/4
9	256-QAM	5/6
10	1024-QAM	3/4
11	1024-QAM	5/6

Table 2.2 – HE-MCS index table nach [17]

Wellenausbreitung, Überlagerungseffekte, Reflexsion, Reflexsion nicht bei Metall

Guard Interval (GI)

Pulimamidi, Nulu, and Tahernezhadi [19] explain the Guard Interval as a cyclic prefix of OFDM symbols before Inter Symbol Interference and through Inter Carrier Intereference. Inter Symbol Interference is caused by multipath delays , where the reflected delayed previous symbol can interfere with the current received symbol[20]. Similarly, Inter Carrier Interference is caused by time-varying channel a longer OFDM symbol duration, that just as an interference with the following OFDM symbol can arise [21].

About the Guard Interval Pulimamidi, Nulu, and Tahernezhadi [19] further list the following. Since the guard interval is to prevent the possible interference on the following symbol, it must be at least long enough so that all channel impulse responses with the resulting delay are caught in the guard interval. The guard interval is then removed again at the receiver. This results in an attentuation of bandwidth which can be described by the following formula:

$$\text{GI\_Bandwidth\_Attentuation} = \frac{\text{OFDM\_symbol\_duration} \times 100}{\text{OFDM\_symbol\_duration} + \text{GI}}. \tag{2.1}$$

Since IEEE 802.11n, a shortened GI of 400 ns is usable, which increases the maximum data rate from 270 Mbit/s to 300 Mbit/s compared to the usual GI of 800 ns [13]. IEEE 802.11ax supports GIs of 800 ns, 1600 ns and 3200 ns to enable better protection against multipath effects in indoor and outdoor communications [23]. better source

No condition for the use of the different GI is mentioned in [23], **mozaffariahrar_survey_2022**, **Rochim** or [15]. Moreover, the sources mentioned only specify a OFDM symbol length of 12.8 µs.

Dual Carrier Modulation (DCM)

In order to introduce additional robustness DCM can be applied to the physical layer since IEEE 802.11ax [14], [22], [17]. Jacob et al. [14] describe DCM as a way to send data twice over two coherent carriers. At the receiver, the data copies are combined with the log-likelihood ratio. This increases the probability of receiving the data.

[17] provides a receiver minimum input sensitivity, which indicates until which RSS a packet is received with a probability of 90 %. The receiver minimum input sensitivity for a BW of 20 MHz is displayed in Figure 2.4. It demonstrates that when using DCM, the receiver minimum input sensitivity can be lower than without using DCM. The effect on the receiver minimum input sensitivity increases as the HE-MCS value increases.

A similar development of the receiver minimum input sensitivity can also be observed for higher BW, except that the lowest value increases with BW.

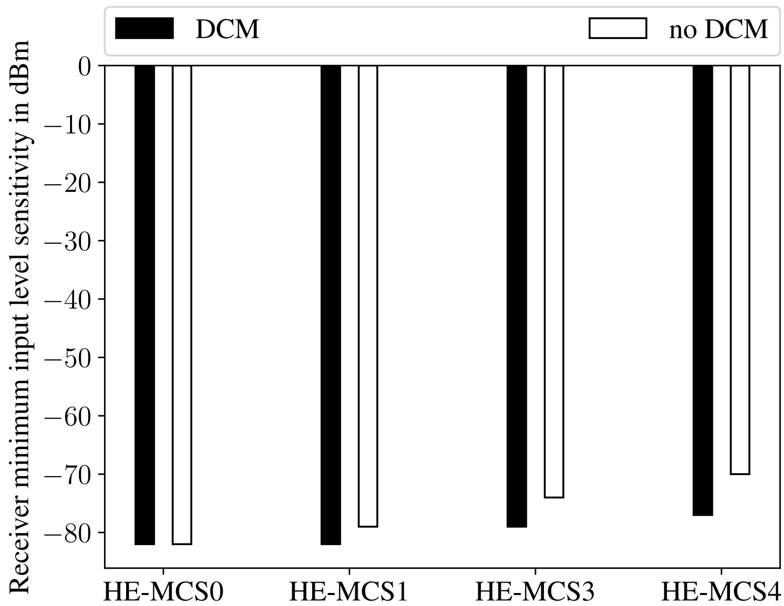

Figure 2.4 – Receiver minimum input level sensitivity for different HE-MCS values according to [17], where packet error rate (PER) is less than 10 %

The higher probability of achieving data is achieve at the expense of the data rate. The same amount of data now takes twice as long to transmit.

[17] lists the theoretically possible data rates. These reveal that the maximum achievable data rate with DCM is only half of the achievable data rate without DCM.

Support for DCM is only optional in the IEEE 802.11ax standard and can only be used for HE-MCS-0, HE-MCS-1, HE-MCS-3 and HE-MCS-4 for 1 . . . 2 spatial transmission streams [17].

Jacob et al. [14] and Triwinarko, Dayoub, and Cherkaoui [22] mention plans, to allow using DCM in the physical layer of IEEE 802.11bd.

BER Ryu

Extended Range

Since IEEE 802.11ax the Extended Range Mode exists, which defines the new HE ER SU Physical layer convergence protocol data unit (PPDU) as physical layer amendment [17] [15]. Deng et al. [23] explains that the HE ER SU PPDU format is intended to extend the range of a single station to access point transmission. This is accomplished, according to the authors, by the PPDU containing a repetition of the HE-SIG-A field.

In addition, the authors explain that preamble is power-boosted, which is limited to 3 dB in [17] [14], to guarantee reliable transmission for longer ranges.

The IEEE 802.11ax [17] standard defines that the HE ER SU PPDU format may only be used when 20 Mhz transmissions with either 242 RU with HE-MCS-0 - HE-MCS-2 or 106 RU with HE-MCS-0 are used on a spatial stream. In addition, one can use DCM.

Optionally, the HE ER SU PPDU may also be transmitted with a GI of 800 ns, where an additional application of DCM is forbidden.

Jacob et al. [14] and Triwinarko, Dayoub, and Cherkaoui [22] add, that it is planned to use the extended range mode also in the IEEE 802.11bd standard.

Multiple Input Multiple Output (MIMO)

In order to further exploit the physical layer capabilities, the single transmitting and receiving antenna systems called Single-Input-Single-Output can be extended to MIMO - systems. Sauter [13] describe the idea behind MIMO as the usage of multiple transmit antennas and multiple receiving antenna. Spatial multiplexing is used so that the transmitted signals from each antenna are reflected differently on objects and can thus be received from different directions at the receiver antennas.

The authors explain that since IEEE 802.11n it is possible to use up to four MIMO streams. This number was increased again to up to eight MIMO streams in IEEE 802.11ax [17]. Since data can be sent simultaneously via each MIMO stream, the theoretical data rate can thus increase proportionally depending on the usable streams. The mechanism is called Single-User (SU)-MIMO [17].

Sauter [13] mentions, that since IEEE 802.11ac it is possible to use Downlink Multi-User (MU)-MIMO, which allows an AP to transmit data to multiple station (STA) via different available MIMO stream simultaneously. According to the authors, MU-MIMO can increase the network throughput. IEEE 802.11ax introduced MU-MIMO in the Uplink direction [17], where multiple STA can transmit data simultaneously to the AP via different available MIMO streams. MU-MIMO DCM only applicable, when RU contains only data for one user [17].

Space-Time-Block-Code (STBC)

Abbas et al. [24] sagt zudem, dass MIMO spatial streams dazu genutzt werden kann, um die Qualität des empfangenen Signals zu verstärken. Das geschieht durch STBC. Dabei werden den Autoren nach redundant copies of data transmitted via different antenna to the receiver. At the receiver the received data copies are combined and a maximum likelihood detector is applied in order to retain a high quality signal [25]. STBC is a technique used in Wi-Fi networks to improve the reliability and robustness of wireless communications. STBC encodes multiple redundant copies of data at the transmit side, which are transmitted in different spatial streams to reduce the effects of fading and interference. At the receiver side, these multiple copies are combined to improve the signal quality and decrease the packet error rate (PER).

Thes results in STBC improving the reliability and robustness of wireless communications. Here, Stamoulis and Al-Dhahir [26] has investigated the potential effect of STBC on Wi-Fi. Their simulations showed thatSTBC can increase the range and robustness for IEEE 802.11a. In addition, the authors concluded that STBC increases the Signal Noise Ratio (SNR) in nearly all cases at the same throughput or even allows higher MCS values to be used, thus allowing a higher throughput at the same SNR.

Ghosh et al. [27] analyzed the error rate performance for increasing number of used antenna and found out, that a lower bit error rate can be achieved when increasing the number of transmit antennas with STBC.

Gast [28] and Sauter [13] mention, that STBC can extend the signal range due to the increased robustness.

IEEE 802.11ax stations can optionally use STBC the following conditions [17]:

- DCM is not applied
- The number of spatial streams is 2
- The GI is not 0.8 ns and the symbol length is not 12.8 µs

[28] states, that STBC is only supported in one fifth of the Wi-Fi CERTIFIED devices. Group addressed frames

HE Capabilities nur so gut, wie das schlechteste Glied

Wi-Fi Data Link Layer

The next layer in the OSI model is the Data Link Layer. The Data Link Layer consists of Medium Access - and Logic Link Control functionalities.

According to Kauffels [12], the medium access control functionalities cover network entry - ,network authentication - and media access methods. The author explains, that every AP send beacon frames periodically to synchronise its stations in the BSS and that the beacon frame contains the Service Set Identifier (SSID), which identifies the BSS or ESS of the station. Sauter [13] adds that a beacon frame contains a 16 bit - long capability information element. Each bit here signals that the AP provides a particular function or has a specific feature.

Kauffels [12] explains the procedure for network entry of a station. A station can use the passive or the active scanning mode. In passive scanning mode, the station listens for a beacon frame in the various transmission channels. Alternatively, in active scanning mode, a station can also send out a probe frame. This can contain an already known SSID to test the presence of the AP. To get an AP in range, the probe-frame can also contain a broadcast SSID that causes all nearby APs to respond. The response of an AP to the probe frame is the probe-response frame, which contains the same information as a beacon frame. With the information from the beacon frame, a station can start the authentication process.

For this process, Kauffels [12] names the two methods Open System Authentication and Shared Key Authentication. Sauter [13] explains that Open System Authentication is based on a device making an authentication request to the AP. If the AP answers with a positive status in the Authentication Frame, the station is included in the BSS. The actual encryption and authentication is then performed by the Wi-Fi Protected Access (WPA) functions. The author points out that Shared Key Authentication is no longer used today.

the IEEE 802.11 standard describes the two media access methods Distribution Coordination Function (DCF) and Point Coordination Function (PCF).

Sauter [13] explains that DCF is based on the media access method Carrier Sense Multiple Access/Collision Avoidance (CSMA/CA). In CSMA/CA a device that is willing to transmit senses in the air transmission medium for a transmitting activity. If no other device is transmitting, the device can transmit. In the case of transmit activity, the terminal must wait at least until the transmission and Distributed Coordination Function Interframe Space (DIFS) are over. Since data transmission via the air transmission medium is very vulnerable to errors, the standard IEEE 802.11 requires that each received packet must be confirmed with an Acknowledgement (ACK) frame. The DIFS ensures that an ACK frame can be sent before another station uses the same channel to send a data frame. To avoid multiple devices transmitting at the same time after DIFS, each ready-to-transmit device determines a random backoff time. The device with the shortest backoff time transmits next and all other ready-to-transmit devices restart the media access procedure. In case two devices start sending next because they both randomly chose the shortest backoff time, the transmitted signal will interfere and the packets will not be answered with an ACK frame. In case of such a faulty transmission, the backoff time of the ready-to-transmit devices can increase exponentially afterwards.

To share the knowledge of a transmission time and the subsequently interframe space, a packet contains a Network Allocation Vector (NAV) that specifies the time the air transmission medium is used.

In various network architectures the "hidden station"-problem may occur. As you can see in Figure 2.5, Station A is not able to sense a transmission of station B and vise versa. In case of simultaneous transmission of both stations, interference around the AP may occur.

Um das hidden station problem zu umgehen kann eine Station nach Sauter [13] Point coordinator ohne Wettbewerb mit optionaler Priorisierung

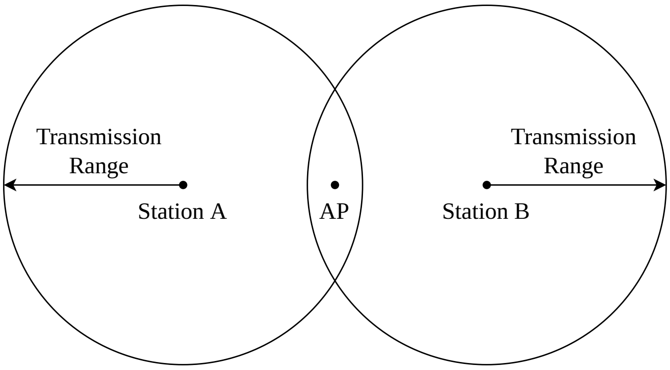

Figure 2.5 – Hidden Station Problem

PIFS interval kürzer, beacon frame CF Parameter set-element

nicht genauer eingehen, weil nicht relevant für die Arbeit? Darf ich das schreiben?

CSMA /CA Point Coordination Function

Sauter [13] DCF oberbegriff für CSMA /CA

Short Interframe Space SIFS ACK Frame

Hidden Station Problem CTS and RTS

IEEE 802.11e DCF erweiterung für Video Streaming

CSMA CA Backoff zeit Network allocation Vector NAV Zeitspanne Datensendungsdauer

MAC Header

Netzeintritt: passives und Aktives Scanning Service Set Identifier Timing Synchronisationsfunktion TSF Timer-Wert

Sauter [13] every package management or usage data send ackknowledgement

Hidden Station Szenario Reservieren RTS CTS meist nicht konfiguriert / ausgeschalten, bei großen Paketen sinnvoll

Authentifizierung - Open System -Authentification - Shared key Authentification (nach neu nicht mehr verwendet

IEEE 802.11ac - Wi-Fi 5

The 5th generation WLAN is IEEE 802.11ac (802.11ac) and operates in the 5 GHz frequency range [29].

According to Perahia and Gong [30], 802.11ac is a further evolution of IEEE 802.11n, where 802.11ac adds to the known bandwidth of IEEE 802.11n of 40 MHz the bandwidths 80 MHz,160 MHz and the interrupted bandwidth of 80 MHz + 80 MHz.

nach Sauter [13] ist die Aufspaltung in zwei 80 Mhz Kanäle sehr nützlich, wenn das frequenzband reservierte Regionen enthält. Dadurch kann ein 160 Mhz breiter Kanal um eine reservierte region des frequenzbandes gebaut werden.

The modulation technique used is OFDM. Additionally, a new MIMO Downlink functionality for multiple users, called DL MU-MIMO, with up to 8 partial streams is introduced according to the authors. Together with the new MCS from 64 QAM to 256 QAM, these three enhancements ensure that a higher data rate can be achieved. The maximum data rate is 6.9 GHz according to the authors.

As declared by Abdelrahman, Mustafa, and Osman [31], the 5th generation of WLAN has made it possible to expect better performance as in addition to a longer communication range compared to the previous IEEE 802.11 standards This statement could be proven at least for indoor range. Dhawankar, Le-Minh, and Aslam [29] were able to demonstrate that 802.11ac with a range of over 60 m enables a longer indoor communication range than previous IEEE 802.11 standards.

new Physical Layer Very High Throughput (VHT) Physical Layer

80 Mhz

Beamforming

IEEE 802.11ax - Wi-Fi 6

The 6th generation of WLAN is IEEE 802.11ax (802.11ax). Khorov et al. [32] reveals what has changed from 802.11ac to 802.11ax. For this, the authors make the following statements.

802.11ax uses the same bandwidths in the 5 GHz range and can also operate in the 2.4 GHz frequency range with a maximum bandwidth of 40 MHz. Similar to DL MU transmission, 802.11ax enables UL MU transmissions. These can also use Orthogonal Frequency-Division Multiple Access (OFDMA) in addition to the already known MIMO of 802.11ac. OFDMA groups the orthogonal frequency subcarriers into Resource Unit (RU)s, which can be selected by the transmitter for optimal transmission to the receiver. This increases the Signal-to-Interference-plus-Noise Ratio (SINR).

An extension in the PHY layer are the new MCS's of up to 1024-QAM. However, these should only be used with very good channel characteristics. For better outdoor communication 802.11ax increases the OFDM symbol duration from 3.2 µs for 802.11ac to up to 12.8 µs and the OFDM Guard Interval from a maximum of 0.8 µs for 802.11ac to up to 3.2 µs.

MIMO und OFDMA MU Streams

BSS Coloring

Backward Kompatibilität über CTS Reservierungen.

Tabelle Vergleich

Parameter	IEEE 802.11ac	IEEE 802.11ax
Frequency bands	5 GHz	2.4 GHz, 5 GHz, 6 GHz
Symbol Length	3.2 µs	12.8 µs
OFDM Subcarrier Spacing	312.5 kHz	78.125 kHz
OFDM Subcarriers in 80 MHz	256	1024
max. MCS	256 -QAM	1024 -QAM
max. GI	0.8 µs	3.2 µs

Table 2.3 – Comparison of IEEE 802.11ac and IEEE 802.11ax

2.4 Related Work

Since my undergraduate thesis [3] about *Wirelessly Networked Coordination of Automatic Section Control for Agricultural Machines* , I have been working on the topic of wireless infield communication (WIC). I conducted both field experiments and simulations to investigate the performance of LoRa as a technology to exchange process data in meshed Automatic Section Control, a prototypical application of connected vehicles in the agricultural domain. A summary of my results is published in a paper [33]. In my undergraduate thesis and paper, I described the current state of research in the field of WIC.

The first research paper on WIC that I found was from Ali [34]. The authors developed a system based on General Packet Radio Service (GPRS) to exchange position data between TMs and combine harvesters to guide empty TMs to a combine harvester.

Smolnik and Lücke [10] describes the research project *5G Netmobil* in which the authors investigated how existing technologies like IEEE 802.11 or 3GPP LTE can be integrated into 5G technologies to enable Agricultural Platooning Services. The research plan was to evaluate the use of User Datagram Protocol (UDP) and Basic Transport Protocol (BTP) to exchange guidance data via the underlying technologies 3GPP LTE and 5G V2X and IEEE 802.11p. The authors implemented a system using 802.11p, as according to their technical analysis, this technology already fulfils the requirements for data rate, latency and the number of participants. The authors report that the project results demonstrated that achieved latencies were five

[3]https://github.com/klautenschlaeger/mvsc Accessed: 5.2.2023

times lower than the defined maximum latency of 50 ms for Agricultural Platooning Services.

Further research on WIC is not based on cellular networks. [7] used IEEE 802.15.4 to implement a prototype of an Agricultural Platooning Service, where the developed system exchanges relevant control data between a leading tractor to guide a following tractor.

Smolnik and Lücke [10] states, that the developed system of Zhang et al. [7] is part of the project *Elektronische Deichsel für landwirtschaftliche Arbeitsmaschinen (EDA)* and it was further improved within the scope of project *Elektronische Deichsel für landwirtschaftliche Arbeitsmaschinen mit Umfeldsensorik und zusätzlichen Geoinformationen (EDAUG)*.

Klingler, Blobel, and Dressler [35] investigated how IEEE 802.11p can be used for WIC. Experiments revealed that data could be exchanged over a maximum range of 1700 m, where Line-Of-Sight (LoS) was lost. But during the measurement in an agricultural work scenario from the corn harvest, there were collapses in the Received Signal Strength (RSS) due to shadowing effects of the machines. The authors point out that the size and shape of the forage harvester can cause intensified shadowing effects.

As of July 2, 2021, the frequency spectrum of IEEE 802.11p in the United States of America, ranging from 5.850 GHz . . . 5.925 GHz, has been split. The upper 30 MHz are reserved for Intelligent transportation systems now. The lower 45 MHz have been released for unlicensed operations [36].

Since the use of IEEE 802.11p has now been newly regulated by the FCC, the WIC project group is looking for an alternative technology that enables WIC.

There are also more developments in the industry field of WIC. In this context, Thomasson et al. [37] describe the John Deere Machine Sync and Case IH V2V systems as follows:

John Deere Machine Sync enables the WIC use cases Process Data Exchange and Agricultural Platooning Service. Liu et al. [8] have extended the system to use Combine Harvesters, adding that the Machine Sync system is based on Metzler, Flohr, and Hoeh [38]'s patent. Smolnik and Lücke [10] adds that John Deere Machine Sync is only available for a subgroup of John Deere machine types and cannot be used with machines of other brands.

Case IH V2V also offers an agricultural platooning service. However, according to the authors, the system can only be used for harvesting and loading scenarios.

Also currently on the market is the Raven Autonomy™ Driver Assist Harvest Solution [4] system from Raven Industries. This system allows the harvester to take control of a TM from a distance of 70 m. The harvester then automatically guides the TM into the perfect position to load the harvested crop onto the TM via the

[4] https://ravenind.com/products/autonomy/driver-assist-harvest-solution Accessed: 5.2.2023

spout. Once the harvesting and loading process is complete, the driver of the TM driver retakes control.

A comparable system is CartACE from AgLeader [5]

The technology used in the mentioned systems is not known. In response to questions about how the systems can be used on farms worldwide and what prerequisites must be created for this, the manufacturers refer to the regional distribution options.

Wireless communication technologies are also used to implement wireless sensor networks in the agricultural domain.

According to Ahmed, De, and Hussain [39], wireless sensor networks in the agricultural domain can be used to monitor soil and water conditions, plant diseases, and farm automation solution or track animals or assets. The authors mention similar requirements for wireless sensor network applications compared to WIC applications. For example, asset-tracking applications require low latency and must support asset mobility. The authors' results indicate that fog computing can lessen the latency and the required bandwidth compared to cloud computing. When a higher data rate is required, the authors recommend wi-fi technologies like IEEE 802.11n or IEEE 802.11ac.

As wireless sensor networks for agricultural applications, they must be able to operate in the same agricultural environment as WIC applications. Brinkhoff and Hornbuckle [40] describe that they expect a limited cellular network coverage and complex outdoor environments with large water areas, different crop vegetation, and other obstacles or various weather conditions. The researchers developed a wireless sensor network based on IEEE 802.11b, where they exchanged data between an AP and multiple stations on a cotton and rice field. The authors report that they easily achieved a communication of 1000 m in a LoS scenario. They mention that different wheater conditions have little impact on communication reliability. A significant influence on the communication range is the height above ground or the crop vegetation, where the authors recommend using at least a height of 0.2 m.

Wi-Fi technologies are also used in various outdoor scenarios. The outdoor performance of Wi-Fi technologies in different use cases and scenarios have been investigated by various researchers. Aust, Prasad, and Niemegeers [41] surveyed past research on outdoor performance of IEEE 802.11 technologies. The authors summarize results of urban, rural, desert or water surface scenarios with different environmental conditions and antenna configurations. I focus on the findings for wi-Fi with omnidirectional antennas in rural areas.

In their general findings, they cite [42] and [43], which name the inter-symbol interference due to multipath effects as main reason for packet losses in wi-fi outdoor communication. The authors conclude, that using directional antennas instead of

[5] https://www.agleader.com/harvest/cartace/ Accessed: 5.2.2023

omnidirectional antennas can lead to fewer multipath effect. Furthermore, the authors add that external wi-fi interference is only expected in urban areas and are not very likely in rural areas.

Due to the experiment results of [44], the authors state that the weather conditions only have a small impact of 1 dB . . . 2 dB on the outdoor communication. These findings are also confirmed by [40] in their experiments on a rice and cotton field.

Paul et al. [45] analyzed the open outdoor performance for different physical layer and MAC layer configurations of IEEE 802.11n. The authors conducted experiments with different omnidirectional antenna constellations and spacings ranging from 0 cm . . . 25.4 cm. They found out, that no positive impact on the communication can be achieved by changing antenna constellations or spacings.

For the MAC layer with its CSMA/CA mechanism, the Aust, Prasad, and Niemegeers [41] state, that the increased propagation delay in outdoor scenarios can cause a higher number of packet collisions. They refer to to findings of [45] and recommend using Block Acknowledgement and Frame Aggregation. These mechanisms introduce a MAC frame overhead, which cost less transmission time than retransmission of a whole frame or a single acknowledgment frame.

Chapter 3

Analyzing Corn Harvest Process Data

To gain a better insight into requirements of the WIC use cases Platooning and Streaming Services, I analysed process data of a corn harvest scenario.

The goal of analysing the corn harvest data was to investigate the machines moving in the working scenarios relative to each other. The machines' speed and distance in tracked harvest platoons data may result in new use case requirements, e.g. latency or communication range of Platooning and Streaming Services. The machinery movement profile can be used to identify when shadowing effects may occur in the work scenario or when machines meet in the field.

To get GPS data of the corn harvest, I collected GPS tracks of a FH and two to three TMs harvesting corn on a field in Germany on two days in September. The workflow for collecting the corn harvest process data was as follows. I handed out the tablets to the drivers, which left the farm with the tablets in the driver's cabs to drive to the field in the morning. The tablets recorded the position and speed of the FH and the TMs every second the whole day. During breaks, the tablets continued to capture the NMEA data stream of their GPS even if the positions and speed did not change.

After recording the process data, I anonymized it. First, I deleted data points of the log files until the recorded accuracy of the following data points was less than 2 m. Then, I replaced the timestamp and the date for all data points with a continuous index.

Then I anonymised the location data by adding a random offset to the GPS coordinates. As a result, this procedure moved the areas to a random location in the world with a continuous index as a timestamp, where the exact date is unknown.

To get a first glance of the recorded data, I built a dashboard with the Python framework *Dash*[6]. I initially plotted all the positions in a polyline for each machine on a map in the dashboard. An added slider allows one to set a time interval that

[6] https://dash.plotly.com/introduction Accessed: 5.12.2022

narrows down the data points for display in the dashboard. In addition, one could select which TMs are displayed next to the FH. For the chosen time interval, the distance and velocity difference between the selected TMs and the FH were plotted in graphs as time histories. In the dashboard, I could get an overview of the machine's behaviour before, during, and after the overloading scenario. The overview shows that a FH is nearly always in the overloading process with a TM. In doing so, the FH may occasionally stay in the same place if the cutter is clogged or there is a transition of TMs where a full TM moves away from the FH and an empty TM catches up to the FH to take over the forage.

UI for selecting the TM to display? Black and White?

A TM is in a platoon with a FH if the distance to the FH is less 10 m and they are moving at nearly the same speed with a maxmimum velocity difference of 5 km/h (1.39 m/s). The distance between TM and FH increases during a turning manoeuvre on the field. Since both machines have different curve radii in a turning manoeuvre, a different machine's speed can be observed to finish turning simultaneously. Smolnik and Lücke [10] also describes these observations and indicates that this speed difference adds a new level of complexity.

A new harvesting process begins as soon as the machines finish turning and are at the beginning of a new lane. Again, the machines drive closely and nearly at the same speed to harvest and overload forage.

Furthermore, another TM can sometimes be close to the FH. For example an empty TM, that waits to work with the FH in the next platoon, drives close behind the current platoon at the same speed to be ready in the vicinity.

Based on the above observations, I developed an algorithm for detecting platooning scenarios in the recorded harvest process data. It uses a weighted sum of distance and speed difference between FH and TM to detect the platooning scenarios.

I determined the weights by Trial-and-Error method, where I set the weights and displayed the found platoons scenarios on the map. Then I adjusted the weights until the found platoons scenarios were correct. For verification purposes, I displayed the found platoons scenarios on the map and confirmed, that the found platoon were correct and the weights were set correctly. Additionally, I implemented the following further verification method whether the found platoons scenarios were correct. I observed that a fully loaded TM leaves the field via one of the field exits to bring the crop to a farm building. Via a check, if a TM has left the field and thereby passed the exit after leaving a platoon, wrongly recognized platoons can be detected. The final weights are $^3/_5$ and $^2/_5$ for the distance and speed difference, respectively.

Add stacked plot, map problem again

After the platoons scenarios were correctly detected, I included the data points before each platoons scenario till a maximum distance of 50 m between FH and TM was exceeded. These data points are also relevant to the requirements because at the beginning of an agricultural platooning service, the FH, as the system leader, must be able to guide an empty TM to the appropriate position for overloading.

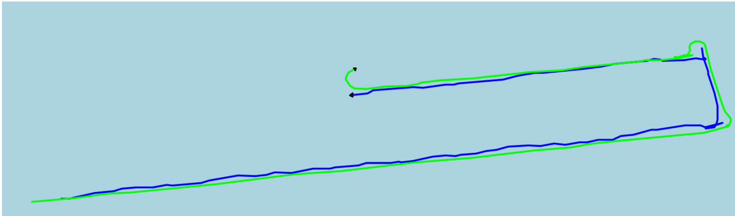

(a) coverage

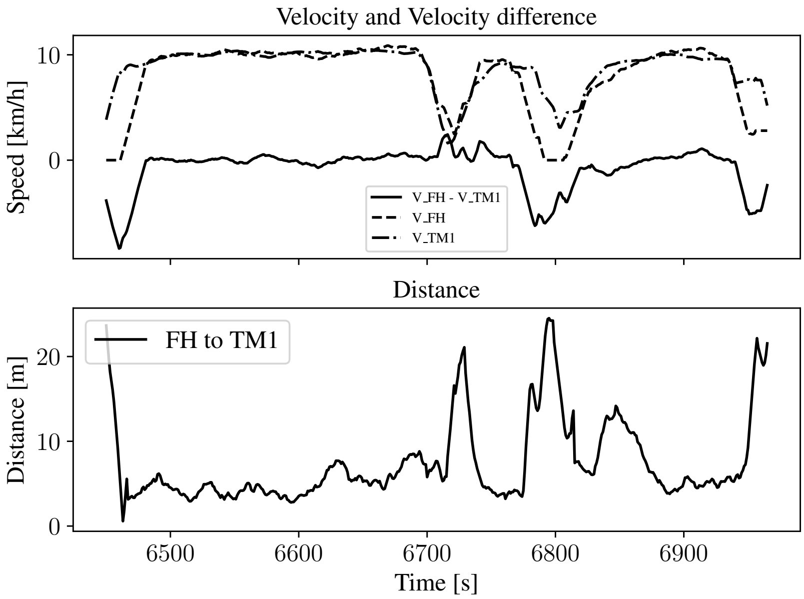

(b) connectivity

Figure 3.1 – Subfigures showing coverage and connectivity for a sample replication at time $t = 0$

For the detected data points of the platooning services from recorded data of the corn harvest, the proportion where the FH and TM move in a specific distance is shown in Figure 3.2. For the same data points, the proportion in which FH and TM move at a given speed is available in Figure 3.3.

These analysing results show that the TM and the FH usually move with a distance of less than 10 m. In addition, the distance can also be higher, e.g. in turning manoeuvres or before the overloading process.

Smolnik and Lücke [10] specifies the required communication range of platooning services in the corn harvest process as less than 30 m.

One notable observation in Figure 3.3 is that the FH and TMs in the corn harvesting platooning scenario often travel at a speed of approximately 10 km/h. This speed is significantly higher than the average speed of 5.6 km/h of a FH in an entire corn harvesting process from [6]. It is necessary to classify that in the year of the

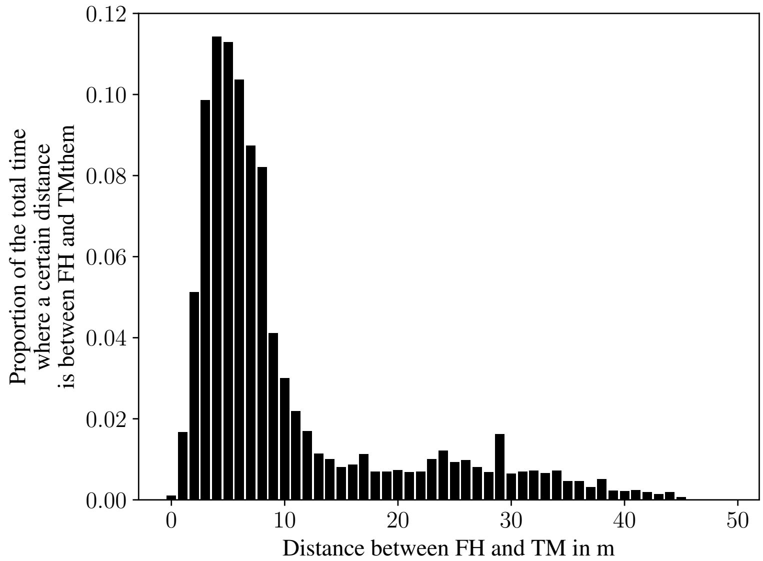

Figure 3.2 – Distribution of time proportions where a given distance was between Forage Harvester (FH) and Transport Machine (TM) in a harvest platoon scenario.

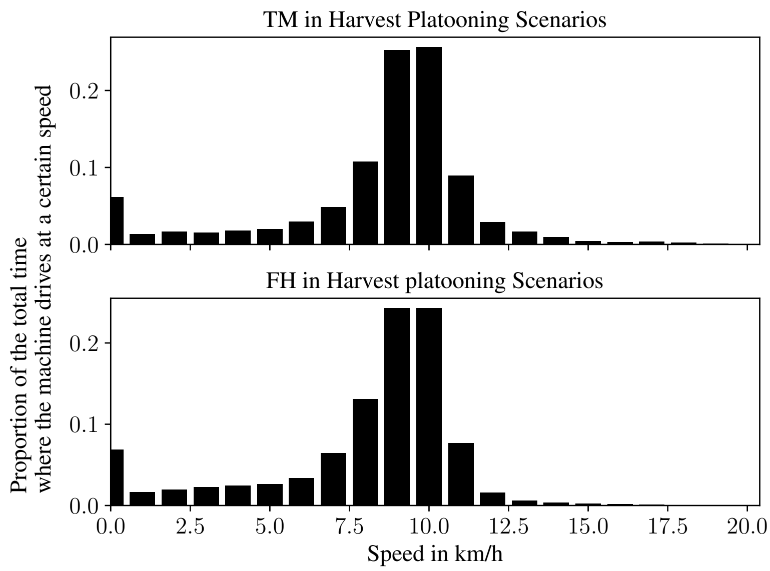

Figure 3.3 – Distribution of time proportions where Forage Harvester (FH) and Transport Machine (TM) drove with a certain speed in a harvest platoon scenario

recorded data was little precipitation, so the corn was not dense and high, and the last speed value is an average value of the entire corn harvest process, which can be calculated from the data in [6]. Nevertheless, the recorded data shows that a platooning service in agriculture must also be designed for higher speeds.

In Figure 3.3 is a local maximum at a speed of 0 km/h. In a harvest platoon scenario, FH and TM can stand still briefly when the cutting device is jammed. The driver's specific actuation usually clears the forage jam of the cutting device so that the platoon can continue its work.

Smolnik and Lücke [10] defines an average speed of 4.5 km/h for the development of platooning services in the corn harvesting process. Depending on the PD, the speed can vary from 2 km/h . . . 6 km/h according to the authors. The authors do not give a basis for the figures. However, the report is from the agricultural machinery manufacturer Claas, which is a major producer of FH worldwide and thus should have expertise in the topic.

Klingler, Blobel, and Dressler [35] investigated the suitability of IEEE 802.11p for WIC. The authors detected that shadowing effects occur in the harvest scenario. The authors explain the effect because another tractor or the spout of the FH was in Line-of-sight (LOS). I reviewed the recorded position data to get an overview of the TM's position relative to the FH in the overloading process. The relative bearing is the angle between the position of the TM, and the heading of the position of the FH. Using the previous position of the FH, the relative bearing between FH and TM can be calculated with the angles α and β in Figure 3.4 as:

$$Relative\_Bearing = \beta - \alpha, \tag{3.1}$$

Assuming that the FH does not move backwards, the relative bearing describes the relative angle from the FH to TM. The result is displayed in Figure 3.5. It can

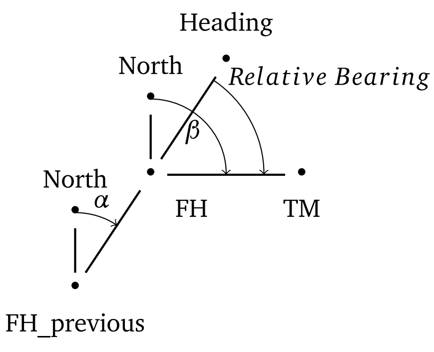

Figure 3.4 – Relative bearing between FH and TM which is calculated using the previous location of FH by using β and α for Equation 3.1

be observed that the TM is mainly close to the FH at an angle of 30° . . . 150° at a distance between 0 m . . . 10 m.

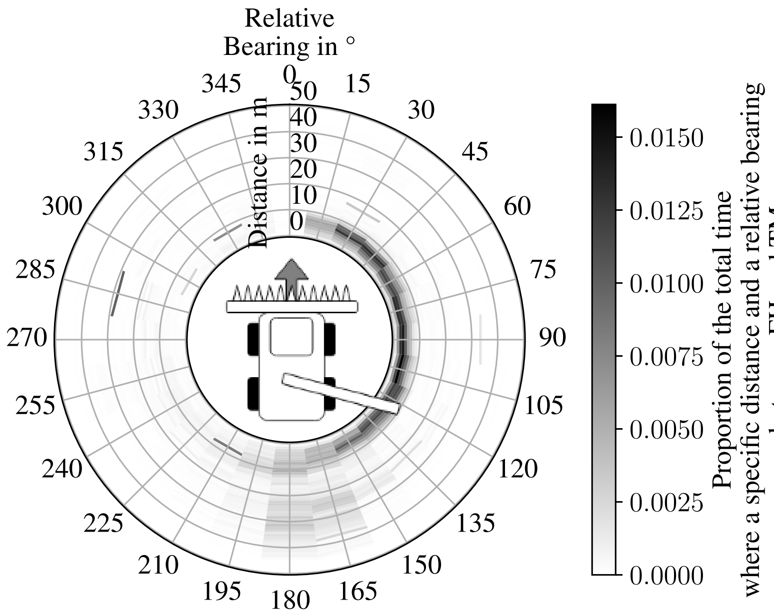

Figure 3.5 – Distribution of time proportion at specific distances and relative bearings between Forage Harvester (FH) and Transport Machine (TM)

In addition, it is noticeable that the machine can also be directly behind the FH. This driving behind each other is common when a new part of the field is being cut in harvesting, as shown in Figure 3.6. When there is a greater distance between TM and FH, the TM is usually behind the FH at an angle of 157.5° . . . 187.5°. At these moments, the TM is empty and closes up to the FH to operate in a new platooning Service together.

Figure 3.6 – Forage Harvester (FH) and Transport Machine (TM) start cutting a new field section

Another notable fact is that the TM hardly ever stayed to the left of the FH. Since the FH often made left turns, the crop was usually already harvested to the right of the FH so that the TM could drive there without running over the crop. On rare occasions, the TM was also to the left of the FH. Such a platooning scenario can be an exception or a driving manoeuvrer to start cutting a new part of the field.

The results reveal only a first impression of the harvest and loading process requirements. More data from around the world must be analyzed to make a general statement. The low rainfall this year has already resulted in a low plant population. This field condition made a higher process speed possible. To make a general statement, I should use data from different years because they can reveal different initial field conditions.

Heading Annahme Vorwärts Fahrt. Ansonsten Überprüfen und nochmal Einzelfahrt plotten und anschauen. Wie oft dreht sich das Heading ? Möglicherweise Rückwärtsfahrt erkennen? Oder WIC Requirements erwähnen?

Chapter 4

Field Measurements

Figure 3.4 shows, that the TM can be positioned at various distances and angles in relation to the FH. For one corn harvest scenario, Klingler, Blobel, and Dressler [35] found out, that the RSS can drop due to shadowing effects caused by the size and shape of the FH and the TM.

In a field experiment, I want to analyze which positions of the TM and FH cause the shadowing effects, which subsequently reduce the RSS and how physical layer parameters like MCS and STBC can used to ensure a low PER.

For the experiment, I will use a Combine Harvester (CH) instead of a FH as it has a similar shape and size as a FH and is available. The TM will be a Tractor pulling a trailer of the type HW80. Both machines will be equipped with a Global Positioning System (GPS) receiver and Wi-Fi devices which record the position, RSS and the PER of the exchanged packets. The CH will be positioned in an agricultural field. The tractor will start 50 m behind the CH, advance to the CH and pass the CH slowly with a speed of 1 km/h . . . 5 km/h (0.28 m/s . . . 1.39 m/s) as shown in Figure **??**. While driving along the specified path, the tractor will mimic various overloading positions, where shadowing effects can occur. After the tractor has passed the CH, it will drive back to its starting position, and the experiment will be repeated with different overloading distances between the CH and the tractor.

During the experiments, GPS receivers at the agricultural machines will record the position and speed of the machines every 1 s.

The Wi-Fi setup consists of a Milesight Industrial Router UR75 **milesight datasheet** which implements the standards IEEE 802.11 b/g/n in the 2.4 GHz band and IEEE 802.11 a/n/ac in the 5 GHz band and IEEE 802.11 a/n/ac in the 5 GHz band. The router is equipped with two omnidirectional antennas for 2.4 GHz and 5 GHz usage. Brinkhoff and Hornbuckle [40] and Paul et al. [45] already found out that placing the antenna higher above ground improves the robustness and communication range of Wi-Fi networks in an outdoor environment. As the regulation in the German Law

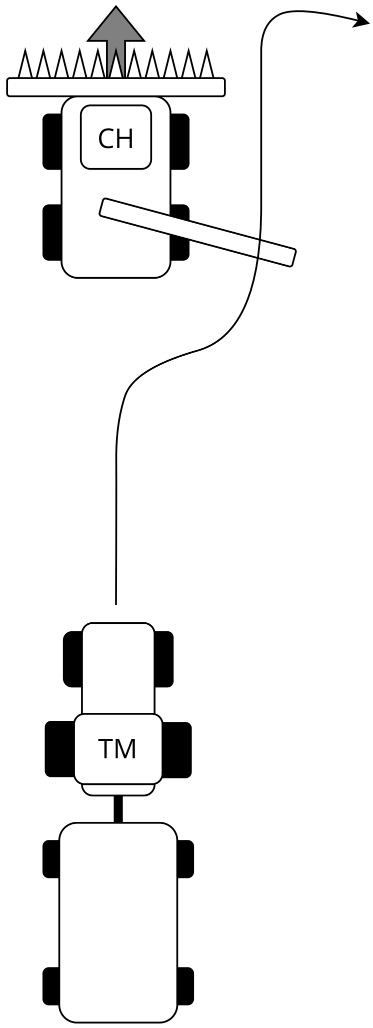

Figure 4.1 – Path around the static Combine Harvester (CH), which the Transport Machine (TM) will drive during the experiment to mimic various overloading positions

StVZO §32 Abs. 2 limits the height of every agricultural vehicle or combination of vehicles to less than 4.0 m, the maximum antenna height is 4 m above the ground. Therefore, I will mount the router on the tractor's roof at a height 4 m above the ground.

I set up two Wi-Fi devices on the CH, which are two UP Squared Board **up_squared_board datasheet** with an Intel AX210 Wi-Fi module **intel_ax210**. Every Intel AX210 Wi-Fi module supports the IEEE 802.11ax standard for 2.4 GHz, 5 GHz and 6 GHz band and is equipped with two antennas, which support omnidirectional transmissions in the 2.4 GHz, 5 GHz and 6 GHz band and have a gain of 5 dB. The boards are mounted on the roof of the CH next to one another at a height 4 m above the ground too.

The router on the tractor sets up a Wi-Fi AP. One of the boards on the CH connects to the AP of the router as a Wi-Fi STA and hosts an iperf3 [7] server. A notebook is connected via LAN to the router and runs an iperf3 client, which connects to the iperf3 server on the CH. The iperf3 client sends 100 Byte UDP packets every 100 ms to the iperf3 server on the CH. The server records the received packets.

Many different Wi-Fi transmissions arise through the iperf3 UDP packets, the Wi-Fi manager of the Milesight Industrial Router, and the Intel AX210 Wi-Fi card. These transmissions can be RTS/CTS, ACK, Data, Beacon or Probe request frame, displayed in Figure 4.2. Through testing, I found out that the Wi-Fi manager of the Wi-Fi devices can apply VHT MCS 0 . . . 9 and STBC as physical layer configurations.

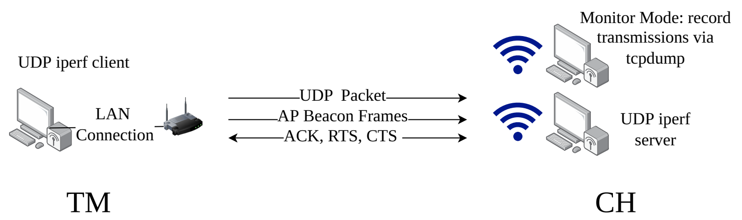

Figure 4.2 – Wi-Fi transmissions between the Wi-Fi AP on the Transport Machine (TM) and the Wi-Fi STA on the Combine Harvester (CH), which are recorded by a third Wi-Fi device in monitor mode on the CH

The other UP Squared Board on the CH uses the Wi-Fi card in the monitor mode and records every transmission in the 5.6 GHz band using tcpdump [8]. Since the UP Squared board is placed next to the other board on the roof of the CH, it can record the same signals the other board receives in the UDP transmission. The tcpdump records are in pcap - format, which can be analyzed using Wireshark[9]. Using Wireshark, I can identify possible retransmissions to calculate a PER. At the same time, the data contains the RSS of each antenna and the physical layer

[7] https://iperf.fr/ Accessed: 8.3.2023
[8] https://www.tcpdump.org/ Accessed: 8.3.2023
[9] https://www.wireshark.org/ Accessed: 8.3.2023

parameters for every transmission, allowing each transmission's robustness to be calculated as a function of the RSS and the physical layer configuration.

In order to get insights on the robustness of different physical layer BWs and used frequencies, the frequency channels in Table 4.1 are configured in the Every specified channel is used separately. To be able to calculate the means and standard deviations of the result for every configuration, the experiment is repeated 5 times for each channel, which means that the tractor drives 5 times the same path, which is displayed in Figure **??**.

BW	Channel number 2.4 GHz	Channel number 2.4 GHz
20 MHz	1	100
40 MHz	3	102
80 MHz	-	106

Table 4.1 – Frequency Channels numbers for 2.4 GHz and 5 GHz for the different bandwidth (BW)s of the IEEE 802.11 standard [46], which can be used for outdoor communication [47], [48] and are configured in the Milesight Industrial Router UR75 for the field experiments.

Describe Mistakes?

Chapter 5

Developed architecture / System design / Implementation / ...

- describe everything you yourself did (as opposed to the fundamentals chapter, which explains what you built on)
- start with a theoretical approach
- describe the developed system/algorithm/method from a high-level point of view
- go ahead in presenting your developments in more detail
- recommended length: approximately one third of the thesis.

Chapter 6

Simulation

Seite 77 von 93 02 simulation.pdf Propagation Model: Two Ray Ground only mathematics Rappaport Jakes Model Three Log Distance

Data Simulation

QUESTIONS open 7 Möglichkeiten outdoor wifi was für Effecte

Robustheit: Matlab? Goodput: ns3 Range: Matlab? Somehow? overview other papers? Enough?

Im folgenden möchte ich den Einfluss der verschiedenen Parameter auf die Robustheit und den Goodput untersuchen. Da wie beschrieben, die vorhandene Technik nicht gezielt angesteuert werden kann, um die Einflüsse der Parameter zu untersuchen, wird eine Simulation durchgeführt. Weitere Vorteile, sind die flexibilität und die Möglichkeit verschiedene Communication Protocol und network protocols zu simulieren **ComparativeStudyKumar**.

OmarHESurvey unterscheidet dabei für die Simulation von HE wireless networks zwischen Link-Level Simulations and System-Level Simulations. Beide Methoden erklären die Autoren, wie folgt.

Link-Level Simulations untersuchen den Autoren nach die performance des HE physical layer für verschiedene physical layer parameter als PER in regards to SNR. Als Beispiel nehmen die Autoren die Simulation von **201** für PER in regards to SNR and chosen MCS.

Für System-Level Simulation benötigt es Abtractionen des physical und des MAC layers, um auf dieser Basis ein system close to real zu simulieren.

Für die Simulation von Wifi gibt es bereits verschiedene Tools, wie z.B. Matlab, ns-2 und ns-3, OMNeT++ oder Qualnet.

SimulationWifiMesh Ns-3 wurde bereits in **ComparativeStudyKumar** und **SimulationWifiMesh** verwendet für die Simulation von Wi-Fi networks. und ist daher für die Simulation von Wifi 6 geeignet. Da ns-3 eine Open Source Software ist, die auch für die Simulation von 802.11ax geeignet ist, wird diese für die Simulation verwendet. Die Simulation wird in der Programmiersprache C++ durchgeführt.

ns-3 Network Simulator

Bei der Wahl der Network Simulator Wifi 6 Implementierungen

Warum nicht was anderes GNS3, MININET, ... ?

In the doc folder of [49] findet man die folgenden Informationen über ns-3. ns-3 is a discrete-event network simulator project, which was founded in 2006. The ns-3 project is open source with a licence based on n GNU GPLv2 compatibility. It aims to procide an open, extensible network simulator for research and educational use. Ns-3 scripts can be written in C++ or Python. ns-API Python uses models in C++ build system Cmake

ATM no pre-built libraries and packages for operating systems

The concept of ns3 is based on the abstraction of simulated systems. For this purpose, the term node was introduced for basic computing devices. The Node class offers the possibility to install protocol stacks and applications or to add peripheral cards and mobility models to the node. Applications are the abstraction of the user-level applications, which represent an activity to be simulated. For this purpose, the applications use resources and functionalities provided by the system software of a node.

Every node gets network access via the Net Device class. The Net Device class represents the physical interface of a node, which can be Network Interface card or peripheral card. The Net Device simulates the software driver and the hardware of the network interface.

Every Net Device is connected to a channel. The channel class represents the physical medium, which is used to transmit data. The channel behaviour is based on the channel model, which may include interference, propagation delay and loss.

Für die aktuelle Version ns-3.37 wird IEEE 802.11ax als Standard im Infrastructure und Adhoc Mode unterstützt [10]. Jedoch ist die Unterstützung für den 802.11ax standard noch nicht vollständig. So kann man bereits DCM und STBC konfigurieren, jedoch findet man die den Kommentar in Zeile 496 von der Datei he-ppdu.cc, dass diese noch nicht in der aktuellen Version 3.37 für beachtet werden [11].

Bei der Untersuchung der Implementierung von 802.11ax in ns-3, fällt auf, dass die Implementierung von 802.11ax in ns-3 auf, dass bereits eine HE ER SU PPDU Preamble implementiert ist, welche jedoch nie genutzt wird und man den Extended Range Mode den nicht aktivieren kann. Die Implementierung von 802.11ax in ns-3 ist also noch nicht vollständig und es gibt noch einige offene Punkte, die in der Zukunft noch implementiert werden müssen.

Black, Gamboa, and Rouil [50] haben eine 3D Visualisierung von ns-3 entwickelt, welche die Simulationen in 3D visualisiert, um die ns-3 simulation scenarios greifbar zu machen. Die grafische Erweiterung der Autoren besteht aus zwei open source

[10] `https://www.nsnam.org/docs/models/html/wifi-design.html` Accessed: 24.02.2023
[11] https://www.nsnam.org/docs/models/html/wifi-user.html Accessed: 24.02.2023

Programmen. Das NetSimulyzer ns-3 module [12] lässt sich in die ns-3 Simulation integieren und baut über die spezifizierten Funktionen und Configurationen eine JSON Datei. Diese beinhaltet alle benötigten Daten für die Visualisierung in der NetSimulyzer [13]

6.1 Data Rate

Using ns-3 I built a simulation to evaluate effect of physical layer configuration on the achievable goodput between two nodes using IEEE 802.11ax Wi-Fi Netdevices to exchange UDP packets in Adhoc Mode. The setup consists of two nodes placed in static positions with a distance of 20 m. I chose the short communication range setup with no simulated interference to enable wi-Fi transmission without any packets lost. Every node is eqipped with a Wi-Fi NetDevice with the following parameters: GI of 3200 ns, a bandwidth of 20 MHz and 2 spatial streams. A Constant Rate Wifi Manager is used to set a constant data rate according to the fixed HE-MCS for data, non-uniform and control data transmissions. The used frequency band is 2.4 GHz or 5 GHz as higher frequencies are less resistant to shadowing and fading and a higher data rate is not needed for the WIC use cases. The Wi-Fi Netdevices operate in the frequency channels specified in Table 6.1, which can be used for outdoor Wi-Fi communication in Germany [47], [48].

As the Wi-Fi standard implements ACKs for every packet, every lost packet is repeated until it is received or the number of retrys is exceeded. Platooning Services are time critical and therefore the number of retrys should be as low as possible. This is why additional retransmission mechanisms like TCP are not needed. Therefore, the chosen transport layer protocol is UDP.

One nodes operate a UDP server and the other one a UDP client. The client sends 1000 Byte UDP packets to the server every 0.1 µs. This packet interval sorgt dafür, dass nach Start der Simulation the packet queue of the client is never empty. The server receives the packets and sends an ACK back to the client.

[12]https://github.com/usnistgov/NetSimulyzer-ns3-module Accessed: 24.02.2023
[13]https://github.com/usnistgov/NetSimulyzer Accessed: 24.02.2023

BW	Channel number 2.4 GHz	Channel number 2.4 GHz
20 MHz	1	100
40 MHz	3	102
80 MHz	-	106
160 MHz	-	114

Table 6.1 – Frequency Channels numbers for 2.4 GHz and 5 GHz for the different bandwidth (BW)s of the IEEE 802.11 standard [46], which can be used for outdoor communication [47], [48]

The simulation runs five times for 5 s for every physical layer configuration. The goodput for every simulation run is calculated by dividing the number of received bytes at the UDP Server by the simulation time. The goodput is then averaged over all simulation runs per physical layer configuration and the confidence interval with a confidence level of 95 % is calculated.

The theoretical data rate for the different physical layer configurations is retrieved from the function ns3::WifiMode::GetDataRate().

In order to verify the simulation software, I used different methods. First, I verified,that the theoretical data rate for the IEEE 802.11 ax physical layer configurations in the simulation is equal to the theoretical data rate specified in the IEEE 802.11ax standard [17].

Additionally, I used the MonitorSnifferRxCallback and the MonitorSnifferTxCallback of the ns-3 WifiPhy class to check the ongoing transmissions. Both Callback functions can be added to WifiPhy objects of WiFi NetDevice and are called every time a packet is received or transmitted at the Wi-Fi Netdevice respectively. The function parameters are Information about the packet, channel frequency and station ID and an instance of the WifiTxVector class. According to **ClassReference**, the WifiTxVector instance describes all parameters of the transmission in acordance to the TXVECTOR field of the IEEE 802.11 standard [17]. Additionally, the function parameters of the MonitorSnifferRxCallback contain the signal strength and the noise power of the received packet.

how to cite?

Using the provided information from the MonitorSnifferRxCallback and the MonitorSnifferTxCallback I was able to comprehend the ongoing transmissions and verify the simulation results.

Überprüfung, Phy-Monitor, Theoretical DataRates

Guard Interval (GI)

In the first simulation I varied the GI of the Wi-Fi Netdevices for different HE-MCS values. The results are shown in Figure 6.1. The achieved goodput is plotted against the theoretical data rate for the different GI values. The theoretical data rate is always higher than the achieved goodput of the UDP applications, because the channel is used for ACK and Adhoc Beacon transmissions as well. Due to these additional transmissions the goodput is lower than the theoretical data rate.

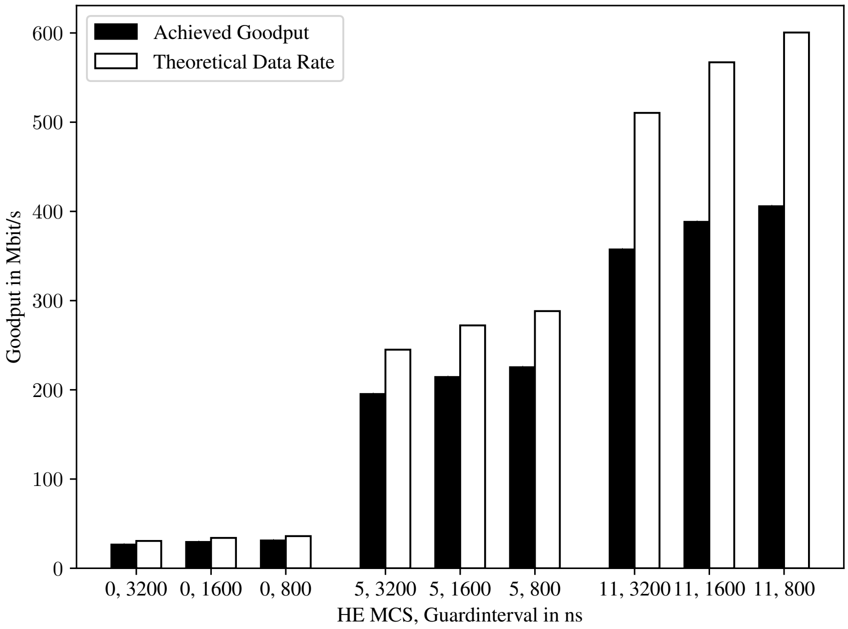

Figure 6.1 – Achieved Goodput and theoretical Datarate of two WiFi 6 stations in Ad-Hoc Mode with 2 Multiple Input Multiple Output (MIMO) streams and a bandwidth of 80 MHz in regards to the number of Multiple Input Multiple Output (MIMO) streams and the chosen HE-Modulation and Coding Scheme (MCS) value

As the GI length increases the achieved goodput deceases. This effect can be characterized by the aforementioned formula. The bandwidth attenuation for the possible GI lengths is displayed in Table 6.2. The effect of the bandwidth attenuation for the different GI lengths can be observed in the mean achieved goodput in Table 6.2, where the decrease of the mean goodput reflects the bandwidth attenuation of the decreasing GI length. A similar effect can be observed whit higher HE-MCS values. **Pravinkumar Patil** similiar sgi and lgi. **Prasad** not similiar sgi and lgi.

Prasad, Patil, GI, Umgang mit Falschaussagen?

GI	Mean achieved goodput	BW attentuation
800 ns	31.15 Gbit/s	94 %
1600 ns	29.47 Gbit/s	89 %
3200 ns	26.52 Gbit/s	80 %

Table 6.2 – bandwidth (BW) attenuation and mean goodput for HE-MCS0 in regards to Guard Interval (GI) length

Multiple Input Multiple Output (MIMO)

Extended Range Mode

In the next simulation I analyzed the effect of the Extended Range Mode on the goodput of the IEEE 802.11ax physical layer. As mentioned in ns-3 Version 3.37, the Extended Range Mode is implemented as an HE Capability with the new extended WifiPreamble. But the new Preamble in the HE ER SU PPDU format is not used in ns-3 version3.37.

As I was using the ConstantRateWifiManager, all paramter for the data transmission are set in the function ConstantRateWifiManager::DoGetDataTxVector(). The function creates a WifiTxVector instance with the parameters of the transmission. There I overwrote the preamble type to the already implemented ns3 WifiPreamble::WIFI_PREAMBLE_HE_ER_SU, when the Extended Range Mode is enabled and conditions for the Extended Range Mode in the IEEE 802.11ax standard [17] are fulfilled. Ns-3 version 3.37 implements ns3::GlobalValue, which allow users to set global values for the simulation, which can be accessed in every class without changing Constructor or function parameters. This leaves the original functionality of the ns3 code intact.

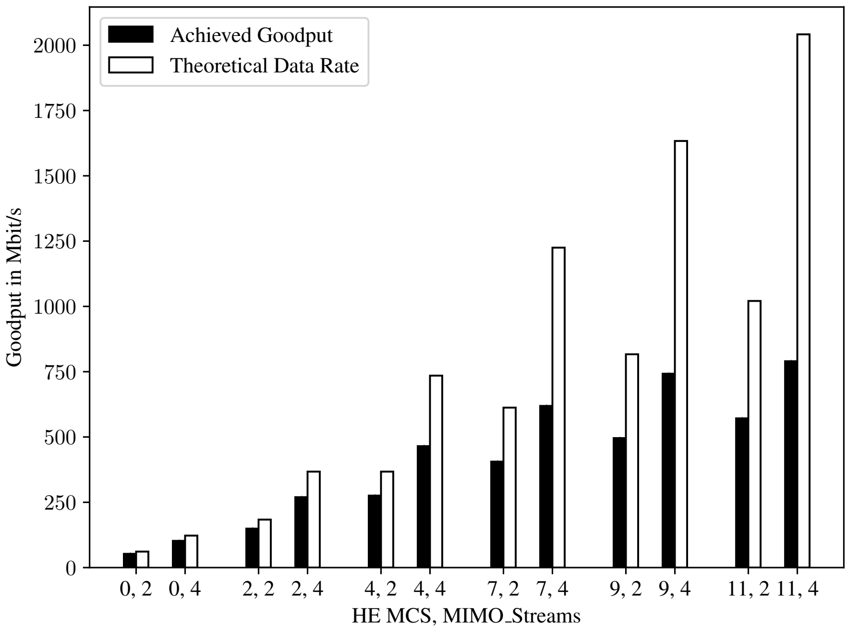

Figure 6.2 – Achieved Goodput and theoretical Datarate of two WiFi 6 stations in Ad-Hoc Mode with a Guard Interval (GI) of 3200 ns and a bandwidth of 80 MHz in regards to the number of Multiple Input Multiple Output (MIMO) streams and the chosen HE-MCS value

I used the ns3::GlobalValue to create an instance named HE_ER_Mode, which is set to true at the start and read in the ns3::ConstantRateWifiManager::DoGetDataTxVector() function to overwrite the preamble type.

Via the MonitorSnifferRxCallback and the MonitorSnifferTxCallback I was able to verify, that the ns3 WifiPreamble::WIFI_PREAMBLE_HE_ER_SU was used for data transmission, when the following conditions were met: a) the Extended Range Mode is enabled, b) the number of spatial streams is 1, c) the HE-MCS value is less than 3 and d) the BW is 20 MHz.

The results of the simulation are shown in Figure 6.3, where the lost achieved goodput is plotted against the theoretical data rate for the different HE-MCS values. The only difference between HE SU and HE ER SU transmissions is the preamble, which repeats the HE-SIG-A field in the HE ER SU PPDU format. This results in a longer transmission time, which reflects in the lower achieved goodput for the Extended Range Mode.

describe lost goodput calculation

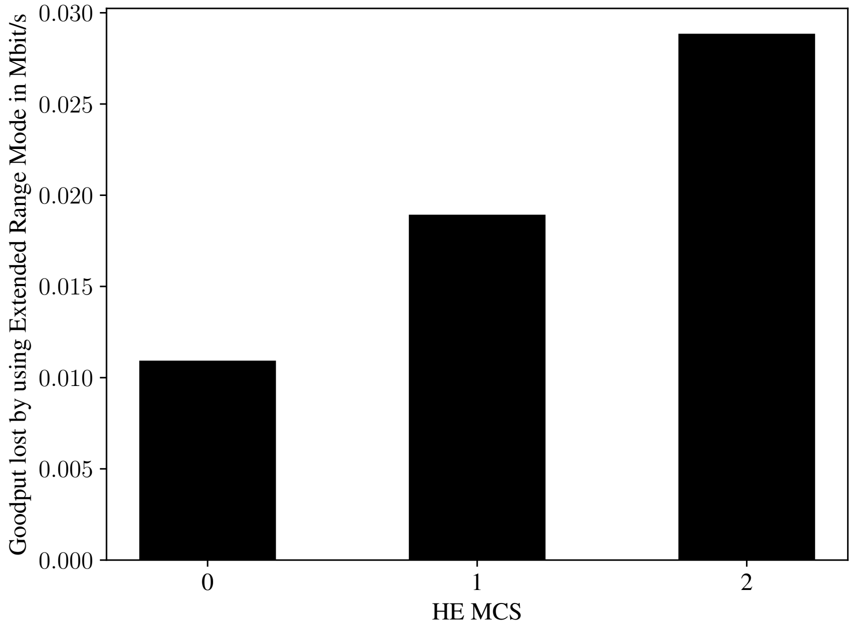

Figure 6.3 – Achieved Goodput and theoretical Datarate of two WiFi 6 stations in Ad-Hoc Mode with a Guard Interval (GI) of 3200 ns and a bandwidth of 20 MHz in regards to the number of Multiple Input Multiple Output (MIMO) streams and the chosen HE-MCS value

The effect increases with smaller packet sizes, because the longer transmission time of preamble is more significant for smaller packets. For higher HE-MCS values more achievable goodput is lost, because longer transmission time for the preamble could have been used more OFDM symbol transmissions, where more data is coded onto a symbol.

Dual Carrier Modulation (DCM)

Using the DCM in the IEEE 802.11ax physical layer has also an effect on the achievable goodput. As aforementioned, the DCM is not supported by ns-3 version 3.37. Therefore, I implemented the DCM for this simulation in the ns-3 version 3.37 by transmitting a payload of twice the size, which represents the original payload and a copy of the original payload for the HE-MCS values 0, 1, 3 and 4, where MCS is allowed. Using DCM, the receiver would apply maximum likelihood decoding to decode the original payload with a higher probability.

The results of the simulation are shown in Figure 6.4, where the lost achieved goodput is plotted against the theoretical data rate for the different HE-MCS values. The theoretical data rate while using DCM is half of the theoretical data rate without DCM, which complies with the IEEE 802.11ax standard [17].

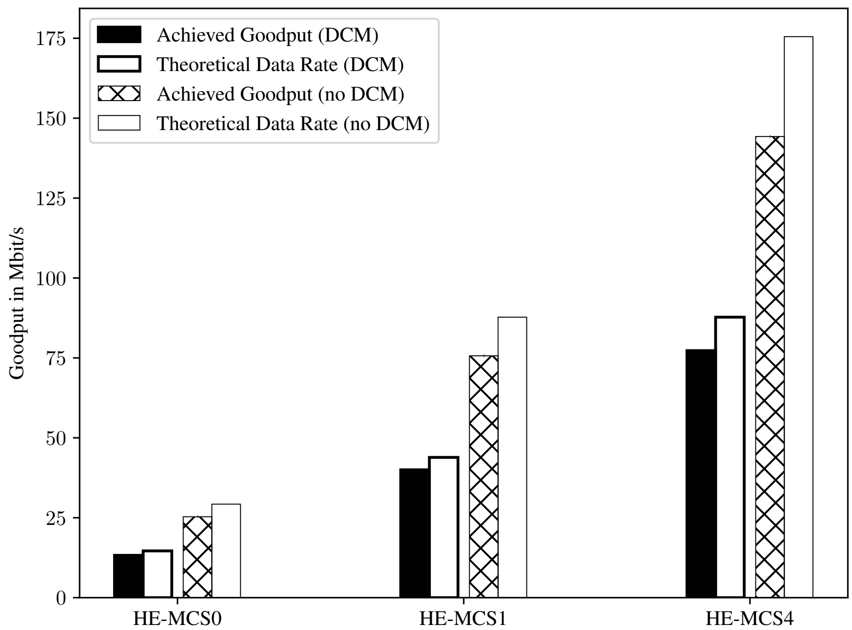

Figure 6.4 – Achieved Goodput and theoretical Datarate of two WiFi 6 stations in Ad-Hoc Mode with for IEEE 802.11ax physical layer parameters of a Guard Interval (GI) of 3200 ns, a bandwidth (BW) of 40 MHz and 2 spatial streams in regards to the number of the chosen HE-Modulation and Coding Scheme (MCS) value and whether Dual Carrier Modulation (DCM) is enabled

The achieved goodput is always lower than the theoretical data rate, because data transmission time is lost to the header overhead and media access time. WiFi access is based on CSMA CA, which means that the stations have to wait for a random time before they can transmit on a free channel. Additionally, the channel can be occupied by ACK or adhoc beacon frames, which also have to be transmitted.

Using DCM increases the ratio of achievable goodput to theoretical data rate, because only one header and one ACK frame is transmitted per 2000 Byte payload and the node has to go to the medium access procudure only once per 2000 Byte payload.

Space-Time-Block-Code (STBC)

Another physical layer parameter, which reduces the theoretical data rate for more robustness is the STBC. As mentioned, ns-3 version 3.37 does not support the STBC for the IEEE 802.11ax standard. Therefore, I reduced the number of MIMO streams from two to one, when the STBC is enabled. STBC would transmit a redundant copy of the data on the second antenna, which would be combined using the space-time block code (STBC) to increase the robustness and reliability of the transmission. The results of the simulation are shown in Figure 6.5, where the lost achieved goodput is plotted against the theoretical data rate for the different HE-MCS values. The theoretical data rate while using STBC is half of the

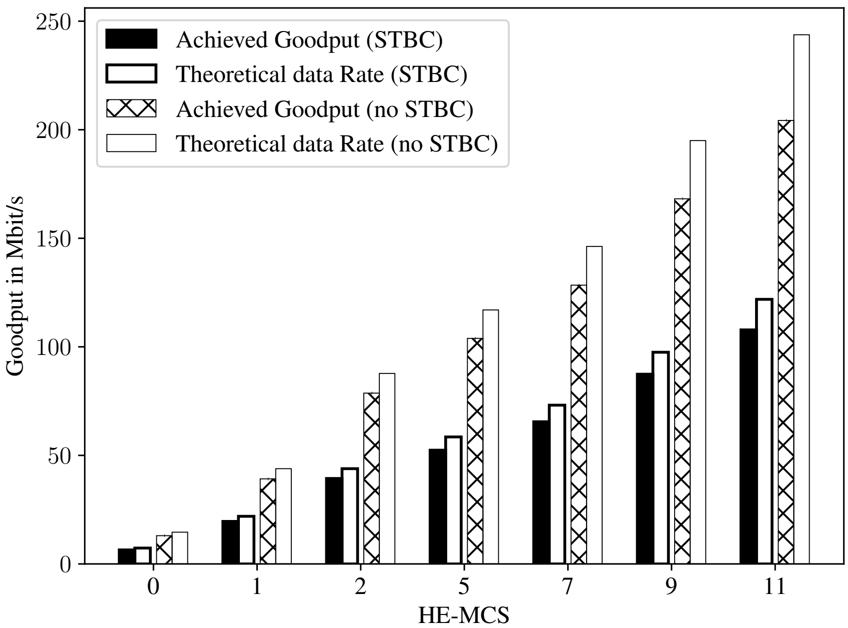

Figure 6.5 – Achieved Goodput and theoretical Datarate of two WiFi 6 stations in Ad-Hoc Mode with for IEEE 802.11ax physical layer parameters of a Guard Interval (GI) of 3200 ns, a bandwidth (BW) of 40 MHz and 2 spatial streams in regards to the number of the chosen HE-Modulation and Coding Scheme (MCS) value and whether Space-Time-Block-Code (STBC) is enabled

Error bars goodput lost

Through the new IEEE 802.11ax standard [17], the Wi-Fi standard has been extended to support more MIMO streams or higher MCS values and use LDPC compulsory for the aforementioned configurations. The effect of more MIMO streams is already known from **Lot of stuff**. LDPC no new effect for data rate, but more robustness which results in a lower PER. Robustness?

6.2 Robustness

The field measurements showed. [10] 3 m corn plants Therefore, the following section focuses on the influence of the different physical layer parameters on the robustness of the IEEE 802.11ax standard Wi-Fi transmissions.

A known simulation tool for wireless communication networks is GNU Radio [14]. GNU Radio is an open-source software development toolkit, which has additional blocks for IEEE 802.11 network simulation, called gr-ieee802-11 [15]. However, the gr-ieee802-11 only supports the IEEE 802.11a, IEEE 802.11b, IEEE 802.11g and IEEE 802.11p. This means, that the gr-ieee802-11 does not support the Extended Range (ER) mode, DCM or STBC. Therefore, I decided that the GNU Radio is not suitable for my simulation.

Accessed necessary?

S, Kuri, and Akhtar [51] cites ns-3 [16], that ns-3 does not implement any frequency-selective fading effects, such as multipath propagation and shadowing. Therefore, the authors decided to use the MATLAB WLAN Toolbox, which is standards-compliant and credible. I also decided to use Matlab because besides [51], [52] and [53] have also considered the MATLAB WLAN Toolbox to be suitable for IEEE 802.11ax simulations.

The MATLAB WLAN Toolbox [17] is a add-on to simulate, analyse, and test of wireless LAN communications systems. The WLAN Toolbox supports a wide range of IEEE 802.11 standards. Since Release R2019b [18], the WLAN Toolbox supports the Signal Recovery, Packet Extension and Physical Layer abstractions to simulation IEEE 802.11ax networks.

My robustness analysis is based on the WLAN Toolbox example wlan/HESUExample [19] to simulate the PER of point-to-point IEEE 802.11ax networks for a specified SNR values.

[14] https://www.gnuradio.org/ Accessed: 14.03.2023
[15] https://github.com/bastibl/gr-ieee802-11 Accessed: 14.03.2023
[16] https://www.nsnam.org/docs/models/html/wifi-design.html Accessed: 13.03.2023
[17] `https://de.mathworks.com/products/wlan.html?s_tid=AO_PR_info` Accessed: 13.03.2023
[18] https://de.mathworks.com/help/wlan/release-notes.html
[19] https://de.mathworks.com/help/wlan/ug/802-11ax-packet-error-rate-simulation-for-single-user-format.html

First, I set the IEEE 802.11ax physical layer parameters using the wlanHEConfig object, where I define the following default parameters:

- GI of 3200 ns
- BW of 20 MHz
- 2 spatial streams
- 2 transmit antennas
- DCM disabled
- STBC disabled
- LDPC enabled
- HE-MCS of 0
- ER mode disabled

use table? Other format?

Next, I chose a channel model to simulate the channel. The WLAN Toolbox supports a wide range of channel models, such as wlanTGaxChannel, wlanTGnChannel, wlanTGacChannel, and wlanTGnChannel. The wlanTGaxChannel model supports 6 different channel models for IEEE 802.11ax networks, named TGax-A, TGax-B, TGax-C, TGax-D, TGax-E, and TGax-F, where the TGax-F channel model is suitable for pseudo-outdoor scenarios [54]. The TGax channel models were used for Matlab Wlan Toolbox simulations by [51], [52] and [53].

[54] and [55] list, that IEEE 802.11ax task group has also implemented the channel models UMa and UMi for outdoor urban scenarios. However, the WLAN Toolbox does not support these channel models and they are intended for urban scenarios, which

As I want to simulate outdoor scenarios, I chose the TGax-F channel model, which is suitable for pseudo-outdoor scenarios [54]. The wlanTGaxChannel model supports configuring the BW, the number of transmit and receive antennas, which I set equal to the configuration of the wlanHEConfig object. [47] and [48] allow outdoor transmission in the frequency range of 5.725 GHz to 5.825 GHz. Therefore, I set the carrier frequency to 5.6 GHz. The TGax-F channel sampling rate is set to 20 MHz, which is the nominal sampling rate for the configured BW of 20 MHz. Additional parameters are left at their default values as they are not relevant for outdoor scenarios. According to the MATLAB WLAN Toolbox documentation [20], the TGax-F channel model has a maximum delay of 1050 ns and root mean square delay spread of 150 ns.

[20] https://de.mathworks.com/help/wlan/ref/wlantgaxchannel-system-object.html Accessed: 13.03.2023

The simulations is based on the procedure 6.1. To get a PER for every SNR value ranging from 0 dB...45 dB, the procedure 6.1 is executed 5 times for 500 packets each. All packet errors are counted and the PER is calculated by dividing the number of packet errors by 500 packets. A mean PER and the confidence interval with a confidence level of 95 % is calculated of the PER values of the 5 iterations.

The procedure 6.1 starts with the creation of a random packet of the specified length of 1000 Byte. The packet is used to create a Wlan waveform based on the physical layer parameters specified in the wlanHEConfig object using the wlanWaveformGenerator function.

The waveform is extended by 50 trailing zeros to ensure, that packet delays can be detected by finding trailing samples unequal to null. When the possible maximum detectable channel delay can be calulated by

$$\text{detectable channel delay} = \frac{\text{Length of trailing zeros}}{\text{Sampling rate}}, \tag{6.1}$$

then 50 trailing zeros match a maximum channel delay of 2.5 µs. As the maximum channel delay of the TGax-F channel model is 1.05 µs, 50 trailing zeros are sufficient to detect the maximum channel delay. I verified Equation 6.1 by comparing the length of the maximum detected packet delay with the maximum channel delay of the TGax-F channel model. The results showed, that maximum detected packet delay is 11 samples, which can be transfered using Equation 6.1 to rounded maximum TGax-F channel delay of 1.1 µs.

Require: Global variable $numPacketErrors$
Create random packet data $txData$ of length 1000 Byte
Create transmission waveform $txWaveform$ from packet data $txData$
$rxWaveform \leftarrow txWaveform$ passed through TGax channel model
Add noise to $rxWaveform$ based on SNR value
Run packet detection on $rxWaveform$
if no packet detected **then**
  $numPacketErrors \leftarrow numPacketErrors + 1$
end if
Detect packet delay $delay$
if $delay > 50$ samples **then**
  $numPacketErrors \leftarrow numPacketErrors + 1$
end if
Steps to recover packet data $rxData$ from $rxWaveform$
if $txData$!= $rxData$ **then**
  $numPacketErrors \leftarrow numPacketErrors + 1$
end if

Algorithm 6.1 – Procedure to detect packet errors

After creating the waveform an appending the trailing zeros, the waveform is passed through the TgaxF channel model to simulate the channel. The output of the channel model is the received waveform, where I added noise to the transmitted waveform based on the specified SNR value and active OFDM subcarriers.

The generated waveform is then passed through the configured wlanTGaxChannel to simulate the channel. The output of the channel model is the received waveform, where I added additive white gaussian noise to the transmitted waveform based on the specified SNR value.

In the next step, the received waveform is passed through the packet detection algorithm, which is based on the WLAN Toolbox example wlan/HESUExample [21] and shown in an abstracted form in **??**. The procedure calls various functions to decode the preamble, header and payload of the received waveform. A packet error is detected, when, no packet can be detected, the packet delay is greater than 50 samples or the recovered packet data is not equal to the transmitted packet data.

Modulation and Coding Scheme (MCS) and Coding Rate (CR)

In a first simulation run, I analysed the influence of a chosen set of HE-MCS values on the PER in regards to the SNR. The results in Figure 6.6 show that the PER decreases with higher SNR for all HE-MCS values. The PER decreases at lower SNR values for lower HE-MCS values. Increasing the HE-MCS value by 2 increases the SNR, where a PER of less than 10 % is achieved, by 5 dB . . . 6 dB.

[21] https://de.mathworks.com/help/wlan/ug/802-11ax-packet-error-rate-simulation-for-single-user-format.html

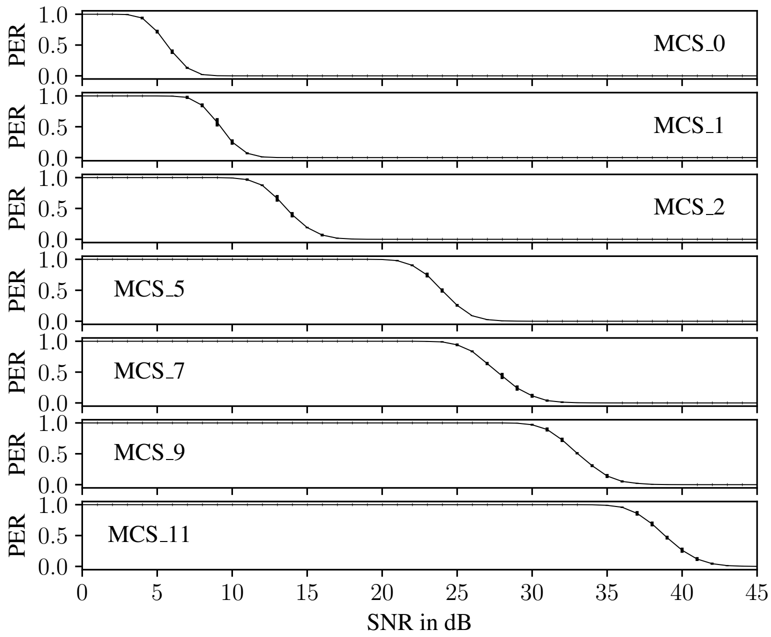

Figure 6.6 – Simulated PER in regards to SNR for chosen HE-MCS values for IEEE 802.11ax physical layer parameters of a GI of 3200 ns, a bandwidth of 20 MHz and 2 spatial streams.

Paul et al. [45] conducted outdoor experiments to analyse the error rate and SNR of different IEEE 802.11n MCS for the communication distances of 300 m, 800 m and 1800 m. Their results show that SNR decreases, when the transmissions range is longer. Additionally, they experienced a higher error rate for higher.

The effect, that the PER decreases, when the a lower MCS or CR is used, is the basis for the design of wifi rate managers. A rate manager is a software component responsible to select physical layer parameters, such as MCS or CR, based on the current network conditions to achieve the best possible throughput. Known rate managers of the linux kernel are the minstrel or the minstrel HT rate manager.

Forward Error Correction (FEC)

Another parameter that influences the PER is the choice of the forward error correction (FEC) procedure. In order to analyse the influence of the FEC procedure on the PER, I simulated the PER in regards to the SNR for HE-MCS 0 . . . 9 and whether LDPC or BCC is enabled. For higher HE-MCS values BCC can be used as LDPC is compulsory, so no comparison of the FEC procedures is possible.

The results are displayed in Figure 6.7. The PER decreases with higher SNR for both FEC procedures for all HE-MCS values as expected. Using LDPC instead of BCC, a PER of less than 10 % can be achieved at 2 dB higher SNR for all HE-MCS values. The effect increases to 3 dB with higher HE-MCS values than HE-MCS 5.

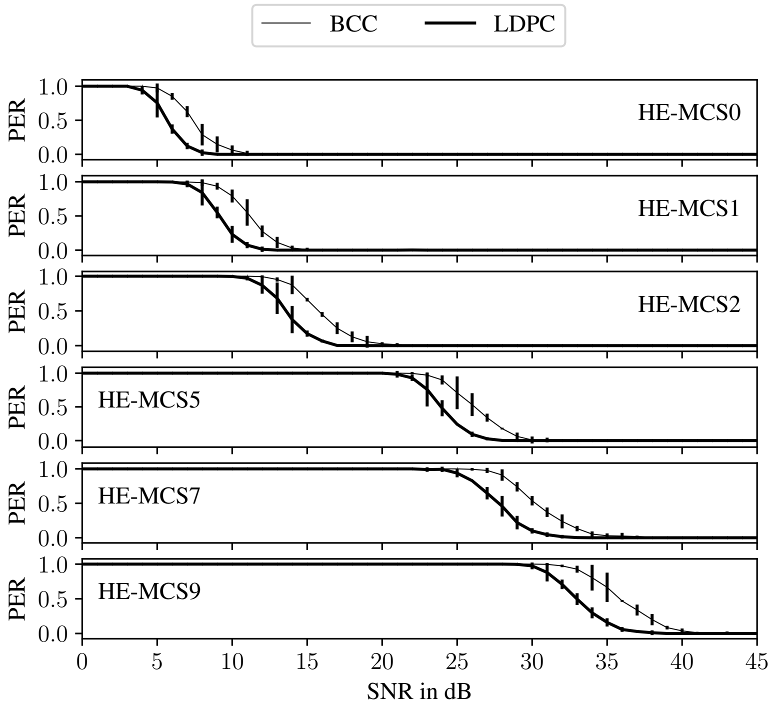

Figure 6.7 – Simulated PER in regards to SNR for chosen HE-MCS values and whether LDPC or BCC is enabled for IEEE 802.11ax physical layer parameters of a GI of 3200 ns, a bandwidth of 20 MHz and 2 spatial streams

Syafei et al. [16] simulated the effect of the FEC procedure on the PER for IEEE 802.11n. They had similar results and state, that using LDPC instead of BCC, a PER of 0.1 % can be achieved at a 3.2 dB . . . 6 dB higher SNR.

According to Tran et al. [56], this effect is also present for IEEE 802.11ac. A PER of 0.1 % can be achieved at a 1.1 dB higher SNR for using LDPC instead of BCC for 64 - QAM. The effect increases to 1.5 dB for 256 - QAM.

Guard Interval (GI)

Robustness against intercarrier interference and intersymbol interference can be achieve by using a longer GI [19]. In order to analyse the impact of the GI on the PER, I simulated the PER in regards to the SNR for different HE-MCS values. The results for a GI of 3200 ns and 800 ns are plotted in Figure 6.8. The PER decreases with higher SNR for all HE-MCS values as expected. Using a GI of 3200 ns instead of 800 ns no significant difference of PER in regards to the SNR can be observed for HE-MCS values lower than 5. Increasing the HE-MCS value, the robustness of the MCS sinks and the effect of the intercarrier interference and intersymbol interference increases. As the maximum channel delay for the Tgax-F channel model is 1050 ns, the channel delay can be longer than the GI of 800 ns. This can result in intersymbol interference, which results in a higher PER for higher HE-MCS values. For HE-MCS5, a PER of less than 10 % can be achieved at 1 dB lower SNR for a GI of 3200 ns instead of 800 ns. The effect increases with higher HE-MCS values.

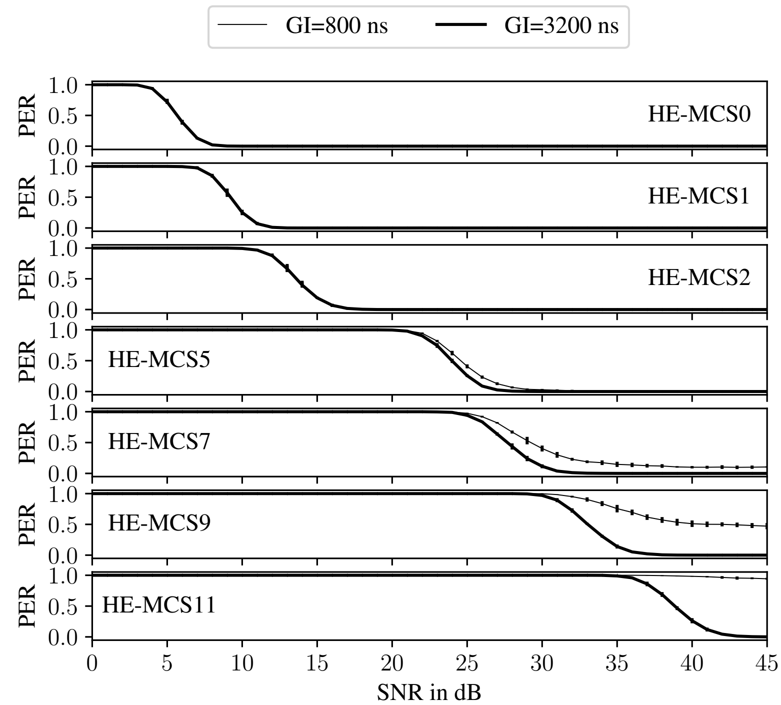

Figure 6.8 – Achieved Goodput and theoretical Datarate of two WiFi 6 stations in Ad-Hoc Mode with a GI of 3200 ns and a bandwidth of 40 MHz in regards to the number of the chosen MCS and CR and whether DCM is enabled

Patil et al. [57] conducted similar simulations for IEEE 802.11n. They agree, that a longer GI can increase the robustness against longer delay spreads as they are in the TGn-E and TGn-F channel models, which are predecessors of the Tgax-F channel model [54].

Dual Carrier Modulation (DCM)

Next, I simulated the PER in regards to the SNR and whether DCM is enabled for the specfied HE-MCS values. Dabei habe ich für die SImulation die möglichen HE-MCS 0,1,3 and 4 aus dem IEEE 802.11ax Standard verwendet.

The results indicate, that using DCM can achieve the same PER at lower SNR values compared to not using DCM. A PER of less than 10 % can be achieved at a 2 dB lower SNR when using DCM. The effect increases to 4 dB for higher HE-MCS4. The results are plotted in Figure 6.9.

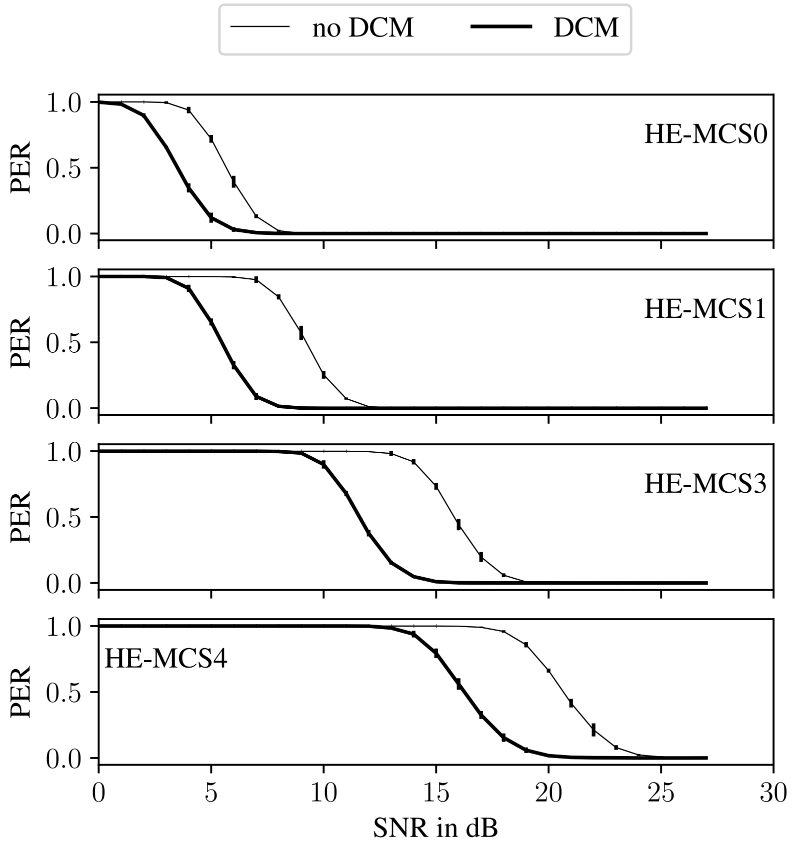

Figure 6.9 – Simulated PER in regards to SNR for chosen HE-MCS values and whether DCM is enabled for IEEE 802.11ax physical layer parameters of a GI of 3200 ns, a BW of 20 MHz and 2 spatial streams

Ryu, Lee, and Kang [58] and Park, Sung, and Ko [59] conducted a similar simulation, where they analyse the bit error rate in regards to the normalized SNR and whether DCM was enabled for rayleigh fading channels. Both authers wraped two Quadrature PSK modulated symbols into one 16-QAM symbol. As Quadrature PSK modulates 2 bit per symbol, the infomation of two Quadrature PSK modulated symbols can be transmitted in one 16-QAM symbol, which encodes 4 bit. The authors transmit the 16-QAM symbols and a redundant copy of the 16-QAM symbols via orthogonal subcarriers. At the receiver the authors combine the copies and retrieve the transmitted information using the Maximum likelyhood criterion. The results of the author show that a better bite error rate can be achieved while applying DCM than sending the information via two Quadrature PSK or 16-QAM modulated symbols without DCM.

Extended Range (ER)

For a HE-MCS 0 and 1 the ER range mode can be applied additional to DCM, when one spatial stream is used [17]. In order to analyse the impact of the ER mode, I set the physical layer parameters to a GI of 3200 ns, a BW of 20 MHz and one spatial streams. For He-MCS 0, 1 and 3 I run simulations, where I enabled the ER mode and compared the PER to the PER of the same HE-MCS values without ER mode.

The results in Figure 6.10 indicate , that the PER is influenced by the ER mode. The difference in SNR with ER mode to without ER mode, where a PER of 10 % is achieved, is 1 dB . . . 2 dB.

Additionally, I simulated the impact of applying the ER mode and DCM for the allowed HE-MCS values 0 and 1. Applying DCM additionally makes the transmission more robust. As it is displayed in **??**, a PER of less than 10 % can be achieved at a

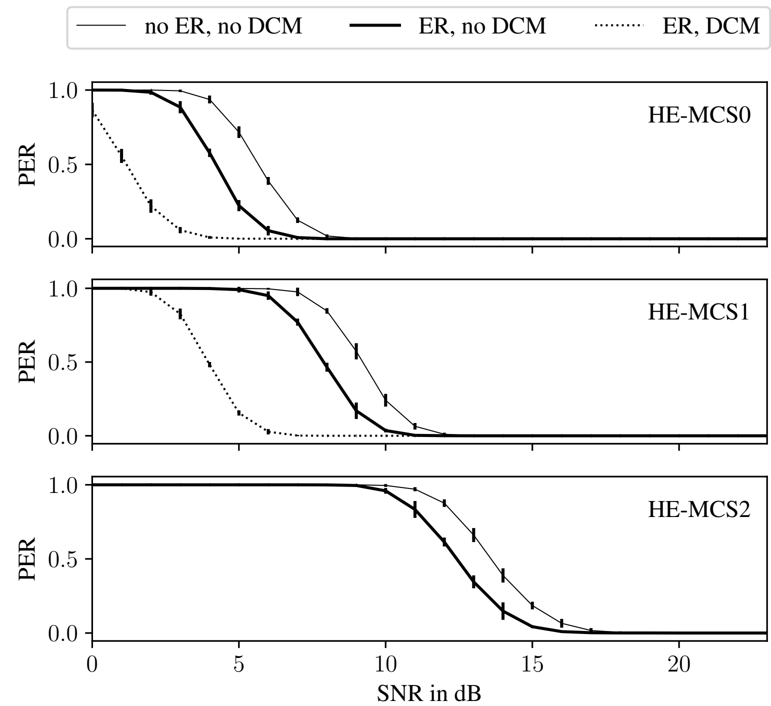

Figure 6.10 – Simulated PER in regards to SNR for chosen HE-MCS values and whether Extended Range or DCM is enabled for IEEE 802.11ax physical layer parameters of a GI of 3200 ns, a BW of 20 MHz and 2 spatial streams

4 dB . . . 5 dB lower SNR when using DCM and ER mode together instead of using ER mode alone.

Jacob et al. [14] conducted a simulation, where they analysed the effect of DCM and ER on the PER for IEEE 802.11bd in vehicular environments to the transmission range. The authors found out, that the using DCM and ER can increase the transmission range for LoS by 65 % for a PER greater than 0.1. After additional analysis with higher vehicle densities, the authors remark, that using DCM and the ER mode cause channel congestion in CSMA/CA based networks with low bandwidths. The authors conclude, that the ER mode and DCM should be used for long range transmissions, where the physical layer parameters can extend the transmission range significantly.

A similar simulation was conducted by Triwinarko, Dayoub, and Cherkaoui [22]. The researchers state, that using DCM and the ER mode results in better PER performance at lower SNR values in LoS and non LoS scenarios.

Space-Time-Block-Code (STBC)

As aforementioned, additional robustness can be achieved by applying STBC. In order to analyse the impact of STBC on the PER in regards to the SNR, I run the simulation for the HE-MCS values 0 . . . 11 with and without STBC.

The results in Figure 6.11 indicate, that the PER is influenced by the STBC mode. A PER of less than 10 % is possible at a 2 dB . . . 10 dB lower SNR when using STBC additionally. The impact of STBC on the PER grows from 2 dB for HE-MCS0 to 10 dB for HE-MCS11.

Stamoulis and Al-Dhahir [26] analysed the impact of STBC on the bit error rate for IEEE 802.11a in regards to the SNR. Their simulation was based on a HiperLAN/2 channel with 2 antennas. They used HiperLAN/2, because it has a similar physical layer as IEEE 802.11a. The authors found out, that applying STBC results in a lower bit error rate for a given SNR value. The authors conclude, that STBC can be used to Santumon [25] and Tarokh, Jafarkhani, and Calderbank [60] conducted simulations, where they analysed the effect of STBC on the bit error rate for wireless communication systems. In general, the authors found out, that STBC can be used to increase the bit error rate for a given SNR value for different MCS values. Additionally, the authors remark, that the impact of STBC on the bit error rate grows with the number of antennas. However, the number of antennas is limited to 2 for IEEE 802.11ax [17].

The robustness analysis results indicate, which PER decreases can be achieved by applying the different phsyical layer parameters. The intensity of the impact varies depending on the environment and the actual communication channel.

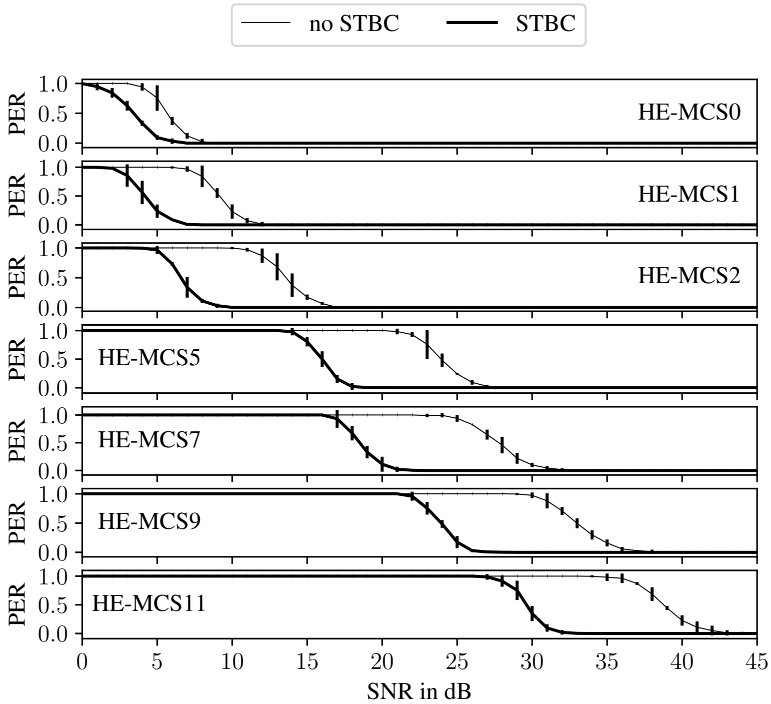

Figure 6.11 – Simulated PER in regards to SNR for chosen HE-MCS values and whether STBC is enabled for IEEE 802.11ax physical layer parameters of a GI of 3200 ns, a BW of 20 MHz and 2 spatial streams

I conducted the same simulations for the frequency band of 2.4 GHz. Using the same physical layer parameters in the 2.4 GHz band achieve a similar PER in regards to the SNR and chosen physical layer parameters as in the 5 GHz band.

But how does the effect of the frequency bands on the PER in regards to the SNR differ? Taking the Friis transmission model [61] into account, the RSS for omnidirectional antennas can be calculated in regard to the distance d, receiving antenna gain G_R, transmitting antenna gain G_T and transmission power P_T as follows:

$$RSS = P_T * G_T * G_R * \frac{\lambda^2}{(4 * \pi * d)^2}. \tag{6.2}$$

When λ is replaced and P_T, G_T, and G_R are set to 1 the following equation can be derived:

$$RSS = \frac{c^2}{(f * 4 * \pi * d)^2}, \tag{6.3}$$

where c is the speed of light and f is the frequency of the transmission. Converting the equation to d it results in the following equation:

$$d = \frac{c}{(4 * \pi * f * \sqrt{RSSI})}. \tag{6.4}$$

The equation shows, that a lower frequency results in a higher RSS for a given distance. This means, that the 2.4 GHz band can achieve a higher SNR for a given distance and noise floor compared to the 5 GHz band. The simulation results can now be used to derive the following conclusion, that a lower PER for the 2.4 GHz band can be accomplished for a given set of physical layer parameters, distance and noise floor.

What should be chosen?

6.3 Platooning Services

After I analyzed the impact on data rate and robustness of physical layer parameter, I will simulate a platooning scenario in ns-3 to find the influence of the found physical layer configuration on the network performance.

Network performance metrics Latency, update received etc.

Zhang et al. [7] defined a data frame of 32 Byte, which includes an identifier, timestamp, Longitude, Latitude, Heading, Speed and Direction. Diese Menge an Daten umfasst eine Grundmenge, welche für die Umsetzung eines Platooning Services ausreichen kann, wie die Autoren zeigen. Schlingmann and Benishek [2] spezifizieren die Datenmenge nicht weiter und weißen darauf hin, dass die benötigte Datenrate für Platooning Services gering ist.

Ich habe für die Simulation von Platooning Services die Datenmenge auf 1 kByte gesetzt. Diese Datengröße ist eine Abstrahierung des Speicherplatzes, welcher möglicherweise für zusätzliche Daten oder Implementierungen von Authentifizierung - und Sicherheitsmechanismen benötigt wird. Im Corn Harvest scenario können zusätzliche Daten z.B. der Füllstand der Transportmachine sein.

Service Discovery

Rebroadcast by Count? additional Traffic

MANET Service discovery

Visualisierung Netsimulyzer

Farbcodes

Harvest State	PD	FH speed
H0	30/ha	10 km/h
H1	40/ha	8 km/h
H2	50/ha	6 km/h

Table 6.3 – Frequency Channels numbers for 2.4 GHz and 5 GHz for the different bandwidth (BW)s of the IEEE 802.11 standard [46], which can be used for outdoor communication [47], [48] and are configured in the Milesight Industrial Router UR75 for the field experiments.

[41] Link Metrics

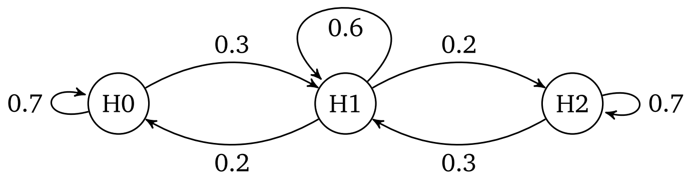

Figure 6.12 – Markov Chain for the states PD 0, 1 and 2, which represent the current Plant Density (PD) and harvest speed from Table 6.3.

Chapter 7

Evaluation

- measurement setup / results / evaluation / discussion
- whatever you have done, you must comment it, compare it to other systems, evaluate it
- usually, adequate graphs help to show the benefits of your approach
- each result/graph must not only be described, but also discussed (What's the reason for this peak? Why have you observed this effect? What does this tell about your architecture/system/implementation?)
- recommended length: approximately one third of the thesis.

Chapter 8

Conclusion

- summarize again what your paper did, but now emphasize more the results, and comparisons
- write conclusions that can be drawn from the results found and the discussion presented in the paper
- future work (be very brief, explain what, but not much how, do not speculate about results or impact)
- recommended length: one page.

Untersuchen, welche Routing protocols

List of Abbreviations

802.11ac	IEEE 802.11ac
802.11ax	IEEE 802.11ax
ACK	Acknowledgement
AEF	Agricultural Industry Electronics Foundation
AP	Access Point
BCC	binary convolutional coding
BSS	Basic Service Set
BW	bandwidth
CH	Combine Harvester
CR	Coding Rate
CSMA/CA	Carrier Sense Multiple Access/Collision Avoidance
DCF	Distribution Coordination Function
DCM	Dual Carrier Modulation
DIFS	Distributed Coordination Function Interframe Space
ER	Extended Range
ESS	Extended Service Set
FEC	Forward Error Correction
FH	Forage Harvester
FMIS	Farm Management Information System
GI	Guard Interval
GPS	Global Positioning System
HE	High-Efficiency
HT	High-Throughput
IBSS	Independent Basic Service Set
LDPC	low-density parity-check
LOS	Line-of-sight
LoS	Line-Of-Sight
M2M	Machine-To-Machine
MCS	Modulation and Coding Scheme
MIMO	Multiple Input Multiple Output

MU	Multi-User
NAV	Network Allocation Vector
OFDM	Orthogonal Frequency-Division Multiplexing
OFDMA	Orthogonal Frequency-Division Multiple Access
PCF	Point Coordination Function
PD	Plant Density
PER	packet error rate
PPDU	Physical layer convergence protocol data unit
PSK	Phase Shift Keying
QAM	Quadrature Amplitude Modulation
RSS	Received Signal Strength
RU	Resource Unit
SINR	Signal-to-Interference-plus-Noise Ratio
SNR	Signal Noise Ratio
SSID	Service Set Identifier
STA	station
STBC	Space-Time-Block-Code
SU	Single-User
TM	Transport Machine
UDP	User Datagram Protocol
V2X	Vehicle-to-everything
VHT	Very-High-Throughput
WIC	Wireless-Infield Communication
WPA	Wi-Fi Protected Access

List of Figures

List of Tables

Bibliography

[1] N. Iglesias, P. Bulacio, and E. Tapia, “Enabling powerful GUIs in ISOBUS networks by transparent data compression,” *Computer Standards & Interfaces*, vol. 36, no. 5, pp. 801–807, Sep. 2014. DOI: `https://doi.org/10.1016/j.csi.2014.01.007`.

[2] N. Schlingmann and M. Benishek, “AEF - Providing electronic communication to the Ag sector for Wireless In - Field Communication,” in *2019 ASABE Annual International Meeting*, Issue: 1901864, Boston, Portugal, Jul. 2019. DOI: `10.13031/aim.201901864`.

[3] N. Schlingmann, H. Schallermayer, J. Witte, and C. Gossard, “Challenges of digital revolution – How the AEF plans to manage interoperability,” in *VDI-Berichte: LAND.TECHNIK AgEng 2017*, vol. 2300, Jan. 2017, pp. 477–484. DOI: `10.51202/9783181023006-477`.

[4] “ICT Facts and Figures 2016,” ITU, ITU-D ICT Statistics 2016, 2016.

[5] H. Seifert, K. Grimm, and M. Schurig, Der Feldhäcksler und was dazu gehört. Wolfratshausen bei München: Neureuter, 1962.

[6] Faustzahlen für die Landwirtschaft, ger, 15. Aufl. Darmstadt: Kuratorium für Technik und Bauwesen in der Landwirtschaft e.V. (KTBL), 2018.

[7] X. Zhang, M. Geimer, L. Grandl, and B. Kammerbauer, “Method for an electronic controlled platooning system of agricultural vehicles,” in *2009 IEEE International Conference on Vehicular Electronics and Safety (ICVES)*, Nov. 2009, pp. 156–161. DOI: `10.1109/ICVES.2009.5400187`.

[8] Z. Liu, S. Dhamankar, J. T. Evans, C. M. Allen, C. Jiang, G. M. Shaver, A. Etienne, T. J. Vyn, C. M. Puryk, and B. M. McDonald, “Automation of Agricultural Grain Unloading-on-the-go,” en, *IFAC-PapersOnLine*, 10th IFAC Symposium on Advances in Automotive Control AAC 2022, vol. 55, no. 24, pp. 248–253, Jan. 2022. DOI: `10.1016/j.ifacol.2022.10.292`.

[9] “Arbeitskräfte in der Landwirtschaft / BMEL (723),” Statistisches Bundesamt: Fachserie 3, BMEL (723) Reihe 2.1.8, 2020, https://www.bmel-statistik.de/landwirtschaft/landwirtschaftliche arbeitskraefte.

[10] I. Smolnik and A. Lücke, “5G NetMobil - 5G Lösungen für die vernetzte Mobilität der Zukunft : Schlussbericht : Teilvorhaben: "Entwicklung eines Parallelen Platooning Systems für den Bereich der Landtechnik unter Verwendung von 5G Technologien"$dSchlussbericht,” [Dissen a.T.W.], Tech. Rep., 2020. DOI: 10.2314/KXP:1757666915.

[11] H. Murcia, “A quadrotor as remote sensor for on-line profile measurement during harvesting process,” Ph.D. dissertation, May 2014. DOI: 10.13140/RG.2.1.1842.3522.

[12] F.-J. Kauffels, Wireless LANs: drahtlose Netze planen und verwirklichen, der Standard IEEE 802.11 im Detail, WLAN-Design und Sicherheitsrichtlinien (Netzwerke), ger, 1. Aufl. Bonn: mitp-Verl, 2002.

[13] M. Sauter, “Wireless LAN IEEE 802.11,” de, in *Grundkurs Mobile Kommunikationssysteme: 5G New Radio und Kernnetz, LTE-Advanced Pro, GSM, Wireless LAN und Bluetooth*, M. Sauter, Ed., Wiesbaden: Springer Fachmedien, 2022, pp. 265–338. DOI: 10.1007/978-3-658-36963-7_4.

[14] R. Jacob, W. Anwar, N. Schwarzenberg, N. Franchi, and G. Fettweis, “System-level Performance Comparison of IEEE 802.11p and 802.11bd Draft in Highway Scenarios,” en, in *2020 27th International Conference on Telecommunications (ICT)*, Bali, Indonesia: IEEE, Oct. 2020, pp. 1–6. DOI: 10.1109/ICT49546.2020.9239538.

[15] M. S. Afaqui, E. Garcia-Villegas, and E. Lopez-Aguilera, “IEEE 802.11ax: Challenges and Requirements for Future High Efficiency WiFi,” *IEEE Wireless Communications*, vol. 24, no. 3, pp. 130–137, Jun. 2017, Conference Name: IEEE Wireless Communications. DOI: 10.1109/MWC.2016.1600089WC.

[16] W. A. Syafei, R. Yohena, H. Shimajiri, T. Yoshida, M. Kurosaki, Y. Nagao, B. Sai, and H. Ochi, “Performance Evaluation and ASIC Design of LDPC Decoder for IEEE802.11n,” in *2009 6th IEEE Consumer Communications and Networking Conference*, ISSN: 2331-9860, Jan. 2009, pp. 1–5. DOI: 10.1109/CCNC.2009.4784735.

[17] “IEEE Standard for Information Technology–Telecommunications and Information Exchange between Systems Local and Metropolitan Area Networks–Specific Requirements Part 11: Wireless LAN Medium Access Control (MAC) and Physical Layer (PHY) Specifications Amendment 1: Enhancements for High-Efficiency WLAN,” *IEEE Std 802.11ax-2021 (Amendment to IEEE Std 802.11-2020)*, pp. 1–767, May 2021, Conference Name: IEEE Std 802.11ax-2021 (Amendment to IEEE Std 802.11-2020). DOI: 10.1109/IEEESTD.2021.9442429.

[18] B. Y. Yacheur, T. Ahmed, and M. Mosbah, "Analysis and Comparison of IEEE 802.11p and IEEE 802.11bd," en, in *Communication Technologies for Vehicles*, F. Krief, H. Aniss, L. Mendiboure, S. Chaumette, and M. Berbineau, Eds., vol. 12574, Series Title: Lecture Notes in Computer Science, Cham: Springer International Publishing, 2020, pp. 55–65. DOI: 10.1007/978-3-030-66030-7_5.

[19] N. Pulimamidi, J. Nulu, and M. M. Tahernezhadi, "Development of a new OFDM transceiver without guard interval," in *2007 IEEE International Conference on Electro/Information Technology*, ISSN: 2154-0373, May 2007, pp. 300–305. DOI: 10.1109/EIT.2007.4374539.

[20] N. S. Ravindranath, I. Singh, A. Prasad, and V. S. Rao, "Performance Evaluation of IEEE 802.11ac and 802.11n using NS3," en, *Indian Journal of Science and Technology*, vol. 9, no. 26, Jul. 2016. DOI: 10.17485/ijst/2016/v9i26/93565.

[21] Van Duc Nguyen and H.-P. Kuchenbecker, "Intercarrier and intersymbol interference analysis of OFDM systems on time-invariant channels," en, in *The 13th IEEE International Symposium on Personal, Indoor and Mobile Radio Communications*, vol. 4, Pavilhao Altantico, Lisboa, Portugal: IEEE, 2002, pp. 1482–1487. DOI: 10.1109/PIMRC.2002.1045425.

[22] A. Triwinarko, I. Dayoub, and S. Cherkaoui, "PHY layer enhancements for next generation V2X communication," en, *Vehicular Communications*, vol. 32, p. 100 385, Dec. 2021. DOI: 10.1016/j.vehcom.2021.100385.

[23] D.-J. Deng, Y.-P. Lin, X. Yang, J. Zhu, Y.-B. Li, J. Luo, and K.-C. Chen, "IEEE 802.11ax: Highly Efficient WLANs for Intelligent Information Infrastructure," *IEEE Communications Magazine*, vol. 55, no. 12, pp. 52–59, Dec. 2017, Conference Name: IEEE Communications Magazine. DOI: 10.1109/MCOM.2017.1700285.

[24] W. Abbas, N. Abbas, U. Majeed, and S. Khan, "EFFICIENT STBC FOR THE DATA RATE OF MIMO-OFDMA," en, 2016.

[25] S. Santumon, "Space-Time Block Coding (STBC) for Wireless Networks," en, *International Journal of Distributed and Parallel systems*, vol. 3, no. 4, pp. 183–195, Jul. 2012. DOI: 10.5121/ijdps.2012.3419.

[26] A. Stamoulis and N. Al-Dhahir, "Impact of space-time block codes on 802.11 network throughput," en, *IEEE Transactions on Wireless Communications*, vol. 2, no. 5, pp. 1029–1039, Sep. 2003. DOI: 10.1109/TWC.2003.816798.

[27] P. K. Ghosh, Manju, K. Gupta, and B. Dey, "Error analysis of multiple rate space-time-block-code (STBC) for MIMO networks," in *Proceedings of The 2014 International Conference on Control, Instrumentation, Energy and Communication (CIEC)*, Jan. 2014, pp. 691–695. DOI: 10.1109/CIEC.2014.6959179.

[28] M. S. Gast, 802.11n: A Survival Guide, en.

[29] P. Dhawankar, H. Le-Minh, and N. Aslam, "Throughput and Range Performance Investigation for IEEE 802.11a, 802.11n and 802.11ac Technologies in an On-Campus Heterogeneous Network Environment," in *2018 11th International Symposium on Communication Systems, Networks & Digital Signal Processing (CSNDSP)*, Budapest, Hungary: IEEE, Jul. 2018, pp. 1–6. DOI: 10.1109/CSNDSP.2018.8471865.

[30] E. Perahia and M. X. Gong, "Gigabit Wireless LANs: An Overview of IEEE 802.11ac and 802.11ad," *ACM SIGMOBILE Mobile Computing and Communications Review.*, vol. 15, no. 3, pp. 23–33, Nov. 2011, Place: New York, NY, USA Publisher: Association for Computing Machinery. DOI: 10.1145/2073290.2073294.

[31] R. B. M. Abdelrahman, A. B. A. Mustafa, and A. A. Osman, "A Comparison between IEEE 802.11 a, b, g, n and ac Standards," *IOSR Journal of Computer Engineering (IOSR-JEC)*, vol. 17, no. 5, pp. 26–29, 2015.

[32] E. Khorov, A. Kiryanov, A. Lyakhov, and G. Bianchi, "A Tutorial on IEEE 802.11ax High Efficiency WLANs," *IEEE Communications Surveys & Tutorials*, vol. 21, no. 1, pp. 197–216, Sep. 2019, Publisher: IEEE. DOI: 10.1109/COMST.2018.2871099.

[33] K. Lautenschlaeger and C. Sommer, "Beyond Sensing: Suitability of LoRa for Meshed Automatic Section Control of Agricultural Vehicles," in *2022 17th Wireless On-Demand Network Systems and Services Conference (WONS)*, Mar. 2022, pp. 1–4. DOI: 10.23919/WONS54113.2022.9764458.

[34] O. Ali, "Multi-agent coordination and control system for multi-vehicle agricultural operations," *Proceedings of the ...*, May 2010.

[35] F. Klingler, J. Blobel, and F. Dressler, "Agriculture meets IEEE 802.11p: A Feasibility Study," in *2018 15th International Symposium on Wireless Communication Systems (ISWCS)*, Lisbon, Portugal: IEEE, Aug. 2018. DOI: 10.1109/ISWCS.2018.8491239.

[36] "Use of the 5.850-5.925 GHz Band," Federal Communications Commission, Rule 2021-08802, May 2021.

[37] J. A. Thomasson, C. P. Baillie, D. L. Antille, C. L. McCarthy, and C. R. Lobsey, “A review of the state of the art in agricultural automation. Part II: On-farm agricultural communications and connectivity,” en, in *2018 Detroit, Michigan July 29 - August 1, 2018*, American Society of Agricultural and Biological Engineers (ASABE), 2018. DOI: `10.13031/aim.201801590`.

[38] P. Metzler, W. Flohr, and M. Hoeh, “System for determining the relative position of a second farm vehicle in relation to a first farm vehicle,” DE102004039460 (B3), Apr. 2006.

[39] N. Ahmed, D. De, and I. Hussain, “Internet of Things (IoT) for Smart Precision Agriculture and Farming in Rural Areas,” *IEEE Internet of Things Journal*, vol. 5, no. 6, pp. 4890–4899, Dec. 2018, Conference Name: IEEE Internet of Things Journal. DOI: `10.1109/JIOT.2018.2879579`.

[40] J. Brinkhoff and J. Hornbuckle, “Characterization of WiFi signal range for agricultural WSNs,” in *2017 23rd Asia-Pacific Conference on Communications (APCC)*, Dec. 2017, pp. 1–6. DOI: `10.23919/APCC.2017.8304043`.

[41] S. Aust, R. V. Prasad, and I. G. M. M. Niemegeers, “Outdoor Long-Range WLANs: A Lesson for IEEE 802.11ah,” *IEEE Communications Surveys & Tutorials*, vol. 17, no. 3, pp. 1761–1775, 2015, Conference Name: IEEE Communications Surveys & Tutorials. DOI: `10.1109/COMST.2015.2429311`.

[42] A. Sheth, S. Nedevschi, R. Patra, S. Surana, E. Brewer, and L. Subramanian, “Packet Loss Characterization in WiFi-Based Long Distance Networks,” in *IEEE INFOCOM 2007 - 26th IEEE International Conference on Computer Communications*, ISSN: 0743-166X, May 2007, pp. 312–320. DOI: `10.1109/INFCOM.2007.44`.

[43] D. Aguayo, J. Bicket, S. Biswas, G. Judd, and R. Morris, “Link-level measurements from an 802.11b mesh network,” vol. 34, Oct. 2004, pp. 121–132. DOI: `10.1145/1030194.1015482`.

[44] K. Chebrolu, B. Raman, and S. Sen, “Long-distance 802.11b links: performance measurements and experience,” in *Proceedings of the 12th annual international conference on Mobile computing and networking*, ser. MobiCom ’06, New York, NY, USA: Association for Computing Machinery, Sep. 2006, pp. 74–85. DOI: `10.1145/1161089.1161099`.

[45] U. Paul, R. Crepaldi, J. Lee, S.-J. Lee, and R. Etkin, “Characterizing WiFi link performance in open outdoor networks,” in *2011 8th Annual IEEE Communications Society Conference on Sensor, Mesh and Ad Hoc Communications and Networks*, ISSN: 2155-5494, Jun. 2011, pp. 251–259. DOI: `10.1109/SAHCN.2011.5984905`.

[46] "IEEE Standard for Information Technology–Telecommunications and Information Exchange between Systems - Local and Metropolitan Area Networks–Specific Requirements - Part 11: Wireless LAN Medium Access Control (MAC) and Physical Layer (PHY) Specifications," *IEEE Std 802.11-2020 (Revision of IEEE Std 802.11-2016)*, pp. 1–4379, Feb. 2021, Conference Name: IEEE Std 802.11-2020 (Revision of IEEE Std 802.11-2016). DOI: `10.1109/IEEESTD.2021.9363693`.

[47] "Allgemeinzuteilung von Frequenzen für die Nutzung in lokalen Netzwerken; Wireless Local Area Networks (WLAN-Funkanwendungen)," Bundesnetzagentur, Vfg. 136 / 2022, https://www.bundesnetzagentur.de -> Fachthemen -> Telekommunikation -> Funk und Frequenzen -> Allgemeinzuteilungen -> WLAN.

[48] "Allgemeinzuteilung von Frequenzen in den Bereichen 5150 MHz - 5250 MHz, 5250 - 5350 MHz und 5470 MHz - 5725 MHz für drahtloser Zugangssysteme einschließlich lokaler Funknetze (WAS/Funk-LANs)," Bundesnetzagentur, Vfg. 136 / 2022, Nov. 2022, https://www.bundesnetzagentur.de -> Fachthemen -> Telekommunikation -> Funk und Frequenzen -> Allgemeinzuteilungen -> WLAN.

[49] Files · ns-3.37 · nsnam / ns-3-dev · GitLab, en.

[50] E. Black, S. Gamboa, and R. Rouil, "NetSimulyzer: a 3D network simulation analyzer for ns-3," en, in *Proceedings of the Workshop on ns-3*, Virtual Event USA: ACM, Jun. 2021, pp. 65–72. DOI: `10.1145/3460797.3460806`.

[51] S. C. S, J. Kuri, and N. Akhtar, "Performance Analysis of Channel-Dependent Rate Adaptation for OFDMA transmission in IEEE 802.11ax WLANs," in *2022 14th International Conference on COMmunication Systems & NETworkS (COMSNETS)*, ISSN: 2155-2509, Jan. 2022, pp. 877–882. DOI: `10.1109/COMSNETS53615.2022.9668513`.

[52] L. Cao, L. Zhang, S. Jin, and S. Roy, Efficient PHY Layer Abstraction under Imperfect Channel Estimation, arXiv:2205.10897 [eess], Oct. 2022. DOI: `10.48550/arXiv.2205.10897`.

[53] S. Jin, S. Roy, and T. R. Henderson, "Efficient PHY Layer Abstraction for Fast Simulations in Complex System Environments," *IEEE Transactions on Communications*, vol. 69, no. 8, pp. 5649–5660, Aug. 2021, Conference Name: IEEE Transactions on Communications. DOI: `10.1109/TCOMM.2021.3079285`.

[54] "IEEE 802.11ax Channel Model Document," IEEE, TGAX channel model document, Sep. 2014, IEEE 802.11-14/0882r4.

[55] H. A. Omar, K. Abboud, N. Cheng, K. R. Malekshan, A. T. Gamage, and W. Zhuang, “A Survey on High Efficiency Wireless Local Area Networks: Next Generation WiFi,” *IEEE Communications Surveys & Tutorials*, vol. 18, no. 4, pp. 2315–2344, 2016, Conference Name: IEEE Communications Surveys & Tutorials. DOI: 10.1109/COMST.2016.2554098.

[56] T. H. Tran, Y. Nagao, H. Ochi, and M. Kurosaki, “ASIC design of 7.7 Gbps multi-mode LDPC decoder for IEEE 802.11ac,” in *2014 14th International Symposium on Communications and Information Technologies (ISCIT)*, Sep. 2014, pp. 259–263. DOI: 10.1109/ISCIT.2014.7011912.

[57] P. Patil, M. Patil, S. Itraj, and U. Bombale, “IEEE 802.11n: Joint modulation-coding and guard interval adaptation scheme for throughput enhancement,” en, *International Journal of Communication Systems*, vol. 33, no. 8, e4347, 2020, _eprint: https://onlinelibrary.wiley.com/doi/pdf/10.1002/dac.4347. DOI: 10.1002/dac.4347.

[58] H.-S. Ryu, J.-S. Lee, and C. G. Kang, “BER analysis of dual-carrier modulation (DCM) over Rayleigh fading channel,” in *International Congress on Ultra Modern Telecommunications and Control Systems*, ISSN: 2157-023X, Oct. 2010, pp. 717–721. DOI: 10.1109/ICUMT.2010.5676558.

[59] K.-h. Park, H.-k. Sung, and Y.-c. Ko, “BER Analysis of Dual Carrier Modulation Based on ML Decoding,” in *2006 Asia-Pacific Conference on Communications*, ISSN: 2163-0771, Aug. 2006, pp. 1–4. DOI: 10.1109/APCC.2006.255858.

[60] V. Tarokh, H. Jafarkhani, and A. Calderbank, “Space-time block codes from orthogonal designs,” *IEEE Transactions on Information Theory*, vol. 45, no. 5, pp. 1456–1467, Jul. 1999, Conference Name: IEEE Transactions on Information Theory. DOI: 10.1109/18.771146.

[61] J. A. Shaw, “Radiometry and the Friis transmission equation,” *American Journal of Physics*, vol. 81, no. 1, pp. 33–37, Jan. 2013, Publisher: American Association of Physics Teachers. DOI: 10.1119/1.4755780.

Todo list